August 2014
Volume 120
Issue 1940
£5.10

www.electronicsworld.co.uk

Electronics WORLD

THE ESSENTIAL ELECTRONICS ENGINEERING MAGAZINE

The cost-effective way of building wireless sensor networks for the IoT

by Digi-key

T&M Supplement
Dedicated supplement on test and measurement

Sensors
Liquid-level sensors for industrial applications

Arduino Projects
Prototyping a keypad and display for the Arduino

August 2014
Volume 120
Issue 1940
£5.10

www.electronicsworld.co.uk

Electronics WORLD

THE ESSENTIAL ELECTRONICS ENGINEERING MAGAZINE

The cost-effective way of building wireless sensor networks for the IoT

by Digi-key

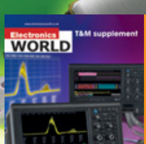

T&M Supplement
Dedicated supplement on test and measurement

Sensors
Liquid-level sensors for industrial applications

Arduino Projects
Prototyping a keypad and display for the Arduino

Cover supplied by
DIGI-KEY CORPORATION
More on pages 8-9

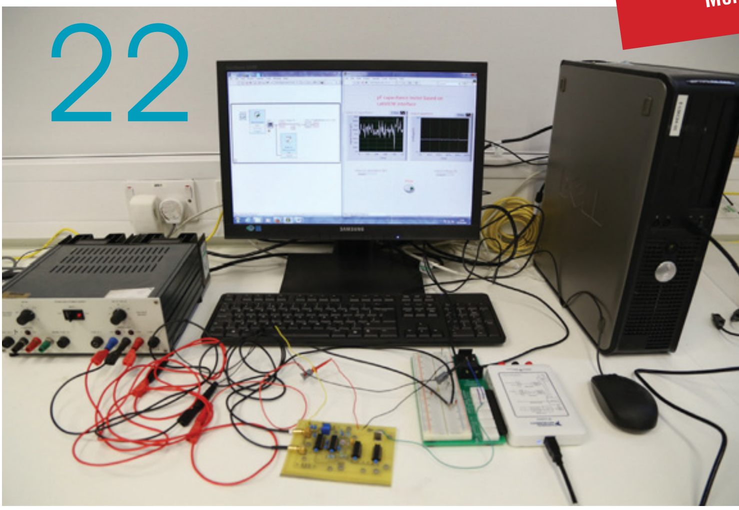

REGULARS

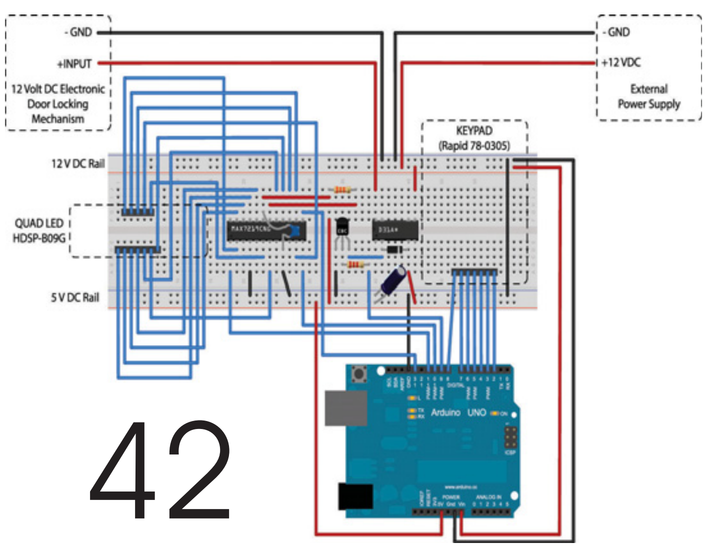

FEATURES

OLSON®

UK's No. 1 IEC Connection

CALL OUR SALES HOTLINE

020 8905 7273

VISA MasterCard Maestro

QMS ISO 9001 REGISTERED FIRM GB 1907

24 HOUR DELIVERY SERVICE

OLSON ELECTRONICS LIMITED
OLSON HOUSE, 490 HONEYPOT LANE, STANMORE, MIDDX HA7 1JX
TEL: 020 8905 7273 FAX: 020 8952 1232
e-mail: sales@olson.co.uk web site: http://www.olson.co.uk

IOT DEVICES OFFER HUGE POTENTIAL FOR COMPONENT MANUFACTURERS

> The main purpose of the IoT is to make sensing ubiquitous at very low cost, resulting in extremely strong price pressure on electronic component manufacturers

The Internet of Things (IoT) device market is expected to grow from $9.5bn in 2014 to $46bn in 2024, opening a huge market for electronic component manufacturers, with most of the added value coming from processing generated data.

"The ratio between electronic components and data processing can reach 1:50 in certain long-term cases," said Dr Eric Mounier, Senior Technology & Market Analyst at Yole Développement.

The main purpose of the IoT is to make sensing ubiquitous at very low cost, resulting in extremely strong price pressure for electronic component manufacturers. Nevertheless, the next five years are expected to be highly rewarding for device makers, with the market predicted to reach $70bn by 2018, before it starts to shrink. This period represents a key window in which manufacturers must seize the opportunity to grab a piece of the IoT business pie.

The IoT is a multi-billion dollar market emerging from several different sectors, including industrial sensors, wearable electronics and home automation among others, which will see strong convergence in the next five years. Three industrial and service areas will be integral to this new market:

- The electronics industry, which manufactures the sensing devices;
- The communication and cloud data storage industry, handling data transmission, storage and processing;
- Service companies, which will handle the data either through processing or by selling it to a third party.

Some companies have already started positioning themselves in these fields. For example, Oracle and Amazon are developing their cloud computing capabilities; Bosch Connected Devices and Solutions and STMicroelectronics have teams dedicated to the IoT; and Google and Facebook are continuously developing their data processing models while looking to acquire companies linked to data gathering. Of course, not all of them will be winners.

The short-term opportunity lies with the electronics industry. Indeed, very strong price pressure is expected for IoT devices, and strong volumes are expected but at very low cost. Even though the general electronics market will experience strong growth, it will come through decreased costs, increased manufacturing capabilities and reduced margins. This trend can already be seen in the MEMS field over the past few years, and will repeat in the future.

The evolution of IoT technologies is mainly focused on heterogeneous integration at device and module levels. The array of technologies available now and soon is immense. Nevertheless, sensing modules' evolution will follow a predefined trend that can be summarized in a series of seven product generations, including large industrial smart sensors, an advanced generation of sensors and polytronics (electronics and systems on flexible substrates).

The Internet of Things roadmap

(Source : Technologies & Sensors for the Internet of Things, Yole Développement, June 2014)

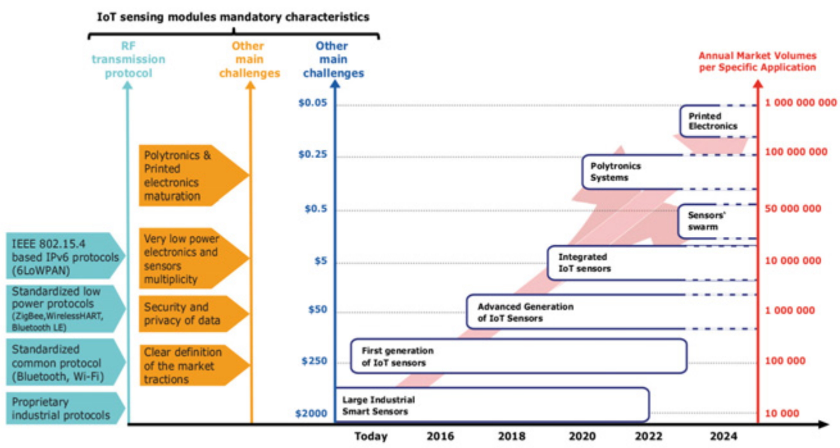

Authors Dr Eric Mounier, Dr Guillaume Girardin and Antoine Bonnabel from French-based market research firm Yole Développement (www.yole.fr) prepared the 'Technologies & Sensors for the Internet of Things' report

EDITOR: Svetlana Josifovska
Tel: +44 (0)1732 883392
Email: svetlanaj@sjpbusinessmedia.com

SALES: John Steward
Tel: +44 (0)20 7933 8974
Email: johns@sjpbusinessmedia.com

DESIGN: Tania King
PUBLISHER: Wayne Darroch

ISSN: 1365-4675

PRINTER: Buxton Press Ltd

SUBSCRIPTIONS:
Subscription rates:
1 year: £59 (UK);
£85 (worldwide)
Tel/Fax +44 (0)1635 879361/868594
Email: electronicsworld@circdata.com

SJP business media

Follow us on Twitter
@electrowo

Join us on LinkedIn

NEW QUANTUM MECHANISM TO TRIGGER THE EMISSION OF TUNABLE LIGHT AT TERAHERTZ FREQUENCIES

Scientists have found that two-dimensional (2D) nanostructures with asymmetric design enable a new quantum mechanism, triggering the emission of tunable light at Terahertz frequencies with unprecedented efficiency. It is hoped the findings will have an impact on photonic and optoelectronic devices across a broad range of applications, including harmless medical imaging and security scanning, and short-range, ultra-fast wireless communications, among others.

The University of Southampton and Imperial College London researchers working on the project found that quantum wells – 2D nanostructures formed of several layers of semiconductor alloys placed on top of each other – can enhance light emission in a spectral range that has proven technologically challenging in the past. Electrons are trapped in the structure and this confinement can be exploited to enhance their capacity to interact with light at given frequencies much lower than the laser frequency at which they are excited: the system emits light by interacting with vacuum fluctuations that permeate space.

"Due to the large oscillating dipole and high density of electrons that characterise these 'artificial atoms' formed of asymmetric 2D structures, the control of light-matter coupling can be greatly enhanced, triggering spontaneous light emission, similar to what occurs in LEDs lamps," said Professor Chris Phillips from Imperial College London. "This new mechanism is perfectly suited for the Terahertz frequency range, which spans from above the current Wi-Fi bandwidth to below the visible light spectrum, where the lack of practical light emitters constitutes a serious technological gap."

Researchers now predict that by shining light on a 2D asymmetric nanostructure with a laser tuned at resonance with the electronic transitions occurring in the nanostructure, this 2D device would emit light at other frequencies, which can be tuned simply by changing the laser power.

"As the 2D nanostructures can be manufactured with an asymmetric design, this allows light to interact with trapped electrons in a way that is not otherwise permitted. This interaction process, leading to the emission of light at lower frequencies, has not been observed in atoms because those are very symmetrical systems and symmetry rules prevent the transitions that trigger this light emission from happening," said Nathan Shammah, from the University's Quantum Light and Matter (QLM) group and co-author of the study.

Optoelectronic device formed of multiple quantum wells emitting terahertz light

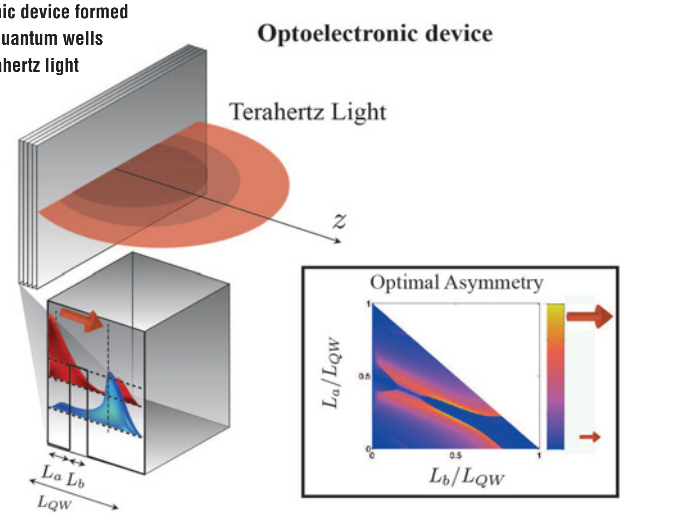

NEW GRAPHENE RESEARCH CENTRE TO OPEN AT THE UNIVERSITY OF SURREY

The University of Surrey will establish a graphene centre within its Advanced Technology Institute (ATI), expanding and consolidating the University's graphene research and manufacturing capabilities.

Through the Centre, the ATI will further its research into the uses and manufacture of graphene across industries, such as high-frequency electronics, flexible and transparent electronics, smart coatings (for example, emissivity and barrier layers), energy generation and storage, electrical interconnect technology, antennas and calibration standards.

"The opening of our new Centre will help ensure that our graphene research is focused on the practical benefits and applications of this material across industries," said Professor Ravi Silva from the University of Surrey and director of the ATI. "This tool is an exciting addition to our existing capabilities. Together with industrial and academic partners, we can combine our expertise in nano-materials and graphene to advance technologies such as electronic devices, supercapacitors, solar cells, OLEDs and printed transistors."

At the heart of the Centre will be the ATI's Photo Thermal deposition technology, which produces large-scale, electronic-grade graphene on wafer substrates. The new tool performs both steps in creating electronic-grade graphene, catalyst deposition and graphene growth, saving the need to transfer the sample between machines. As the sample is kept in a vacuum, the grown material is of higher quality. Additionally, the process allows high volume production in an industrial environment.

The Centre has received funds of over £1.2m from the Engineering and Physical Sciences Research Council (EPSRC), in collaboration with BAE Systems, Tata Steel, Airbus Defence and Space, Intel, M-Solv, Thomas Swan, DSTL and the National Physical Laboratory (NPL). Academic partners include the Universities of Cambridge, Oxford, Manchester, Imperial, Exeter, Trinity College Dublin and Aristotle University of Thessaloniki, Greece, who will help to ensure that the graphene technologies developed at the Centre are used by industry.


FREE SHIPPING
ON ORDERS OVER £50!*
DIGIKEY.COM
ONE STOP
Prototype to Production®
Search
Parts
Content
GO
In Stock
Lead free
RoHS compliant
Login
Register | Why Register?
United Kingdom | 0800 587 0991
GBP | Change Country
Online Ordering
Order Status
Newest Products
Product Index
Supplier Index
Catalogue
Resources
TechXchange℠ Community
Supply Chain HQ℠
Need Help?
WORLD'S LARGEST SELECTION
of electronic components AVAILABLE
for immediate shipment!
Broadest BOM Coverage In The Industry
49%
DIGI-KEY
15%
5%
4%
2%
1%
Other Distributors
BEST-OF-CLASS: E-COMMERCE/ONLINE BUYING
Source: 2014 Design Engineer and Supplier Interface Study, Hearst Business Media Electronics Group
Digi-Key® CORPORATION
0800 587 0991 • 0800 904 7786
DIGIKEY.CO.UK
1,000,000+ PRODUCTS IN STOCK | 650+ INDUSTRY-LEADING SUPPLIERS | 3.9 MILLION PARTS ONLINE
*A shipping charge of £12.00 will be billed on all orders of less than £50.00. All orders are shipped via UPS for delivery within 1-3 days (dependent on final destination). No handling fees. All prices are in British pound sterling and include duties. If excessive weight or unique circumstances require deviation from this charge, customers will be contacted prior to shipping order. Digi-Key is an authorized distributor for all supplier partners. New product added daily. © 2014 Digi-Key Corporation, 701 Brooks Ave. South, Thief River Falls, MN 56701, USA
ecia
ecsn
member
CEDA

DISCRETE OR INTEGRATED? INVESTIGATING THE DESIGN OPTIONS FOR WIRELESS NODES IN THE IOT

The Internet of Things is bringing a greater focus on the most cost effective way to build a wireless sensor network, from the node to the gateway. There are numerous engineering tradeoffs involved, particularly for the performance, cost, and power consumption of the wireless sensor node, finding a balance between a highly integrated device and a discrete implementation.

Other key factors in the choice between an integrated implementation and the discrete version are the frequency band and protocol, and the size of the application code. Popular protocols, such as Wi-Fi or ZigBee in the 2.4 GHz unlicensed frequency band, are high volume applications that lend themselves to high levels of integration. However, the cost sensitivity of these markets means that the on-chip memory is optimized for the protocol stack. This may reduce space for user code, requiring an additional processor. This can eliminate the advantage of using an integrated device. Similarly, custom protocols and applications in the 800-900 MHz band for longer-range links may not have enough volume to warrant an integrated solution, so a discrete implementation may be more cost effective.

Rich Miron, Technical Content Engineer

While simple integrated wireless sensors are abundant, growth in the Internet of Things demands increased network management and security, changing the design options for the system architecture. At the same time, serial interfaces are cost-effective enough to be used for applications such as sensor networks where high-speed data is not necessary.

Wireless sensor nodes

A wireless sensor node generally consists of a sensor, a data converter, microcontroller, a wireless protocol engine and MAC transceiver, and the physical PHY radio front end. For applications requiring longer range or operating in noisy industrial environments, a separate power amplifier could be required.

There are several options for this type of integration. Integrating a sensor with a microcontroller may provide enough spare cycles and memory to implement a protocol stack, particularly for simple protocols in the 800 MHz ISM band.

In other architectures, several sensors may be linked up to a single controller or digital signal processor (DSP) that needs to continually monitor a number of variables. This may limit the cycles available to handle the protocol stack, so a separate protocol engine integrated with the MAC can provide more efficient resource utilization. Previously, having the RF front end separate from the MAC allowed an RF process to be used for a more efficient front end, providing higher performance. However, with the 65 nm process technologies and below, CMOS RF is eminently suitable for integration alongside the MAC, driven largely for the demand for 2.4 GHz Wi-Fi and ZigBee chips. However, chip companies have added the flexibility to support similar industrial protocols such as WirelessHART in the devices. If the application demands a longer range, adding a discrete power amplifier alongside an integrated chip is a common solution.

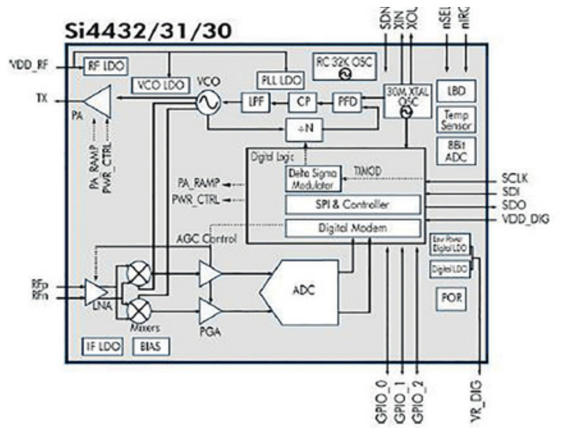

Figure 1: The Si443x family of devices supports frequencies continuously from 250 MHz to 960 MHz in 156 Hz or 312 Hz steps and antenna diversity architectures that are not possible in a more integrated device.

Integration of interfaces such as SPI and I2C has simplified the development of discrete systems combining a transceiver and a separate microcontroller. This is common on many devices, simplifying system integration.

The AT86RF32 from Atmel is a separate transceiver that supports ZigBee, 6LoWPAN, RF4CE, SP100, WirelessHART and other ISM applications. The radio transceiver is a true SPI-to-antenna solution, with all RF-critical components except the antenna, crystal and de-coupling capacitors integrated on-chip. Reference designs exist outlining how to interface to Atmel's 8-bit AVR microcontrollers such as the ATMEGA88.

Discrete RF transceiver front ends can also be used for different architectures such as variants of the MIMO multiple antenna design.

The Si4431 from Silicon Labs is a standalone RF transceiver that supports frequencies continuously from 250 MHz to 960 MHz in 156 Hz or 312 Hz steps and antenna diversity that may not be available in more highly integrated devices.

The Si4431's high level of integration offers reduced BOM cost while simplifying the overall system design. The extremely low receive sensitivity (–121 dBm) coupled with the +20 dBm output power ensures extended range and improved link performance. Built-in antenna diversity and support for frequency hopping can be used to further extend range and enhance performance.

Additional system features, such as an automatic wake-up timer, low battery detector, 64 byte TX/RX FIFOs, automatic packet handling, and preamble detection reduce overall current consumption and allow the use of lower-cost system MCUs. An integrated temperature sensor, general purpose ADC, power on-reset (POR), and GPIOs further reduce overall system cost and size.

Integrated devices

Integrated solutions are appealing for potentially lowering the overall bill of materials cost, but there are several elements to keep in mind.

One of these is the overall architecture for the sensor nodes. Integrated transceivers have a processor, often 32-bit, and memory architecture optimized for the wireless protocol. Using a 32-bit architecture allows the integrated device to use optimized 32-bit code for the protocol stack as in the JN5168 from NXP.

The use of integrated transceivers with optimized 32-bit code makes it easier to develop and debug applications than custom or assembler code, and provides a higher quality solution. It also allows the system engineer to include Internet protocols such as TCP/IP, which allows the node to be accessed directly from the Internet rather than through a dedicated gateway. This reduces the complexity involved with managing a large distributed sensor network.

However, there is limited opportunity to add additional functions to the device, which can limit the possible cost savings. Keeping the protocol stack and networking element separate from the rest of system allows more security and reliability, as there is less potential for problems between the user code and the network stack. It is also increasingly important to include security elements in the network stack to prevent unauthorized access.

One integrated device may have sufficient spare clock cycles and memory to be able to support one or two sensors, as well as the wireless link, but may not be able to support more sensors. This can impact the potential for upgrading or enhancing the system with additional sensors at a later date. It can also restrict the ability to upgrade the system with new versions of the protocol that can provide higher performance, allow for a lower power link for the same data rates, patch previously unknown security holes, or upgrade the level of security in the device. Spare memory is often used to support downloads of code over the air, allowing the system to be upgraded remotely. Using this extra space for user application code can compromise the aforementioned upgradeability, which can be vitally important.

Integrated solutions are also possible in the lower frequency bands for simpler fixed functions such as security systems or simple measurements.

The ADF7020 from Analog Devices is a low-power highly integrated FSK/ASK/OOK transceiver, designed for operation in the license-free ISM bands at 433 MHz, 868 MHz, and 915 MHz and including an integrated temperature sensor.

An on-chip ADC provides data from an integrated temperature sensor, external analog input, battery voltage, or the RSSI signal, providing savings on an ADC in some applications. The temperature sensor is accurate to ±10°C over the full operating temperature range of –40°C to +85°C. Accuracy can be improved by doing a 1-point calibration at room temperature and storing the result in memory.

A complete transceiver can be built using a small number of external discrete components, making the ADF7020 very suitable for price-sensitive and area-sensitive applications. The transmitter block on the ADF7020 contains a VCO and low noise fractional-N PLL with an output resolution of <1 ppm. This frequency agile PLL allows the ADF7020 to be used in frequency hopping spread spectrum (FHSS) systems.

Conclusion

A common architectural choice is to have an integrated transceiver for a protocol such as ZigBee, Bluetooth or Wi-Fi handling the network access for the node, with a separate microcontroller with integrated ADC such as the 8-bit AVR ATMEGA88 from Atmel or the 32-bit ARM Cortex-M0+ Zero Gecko EFM32ZG110F32 from Silicon Labs and external memory to handle multiple sensors. This supports more flexible implementation of network protocol, upgrades for performance or security, and the ability to potentially support new versions of a wireless standard. This also allows the code in the sensor controller to be upgraded separately and for additional security to be included such as an AES128 encryption engine to support a higher security link for the Internet of Things. Being able to handle the encryption, device and network security, protocol stack and network management that are increasingly demanded by IoT designs is still a tall order for a low cost, low power microprocessor core in an integrated device.

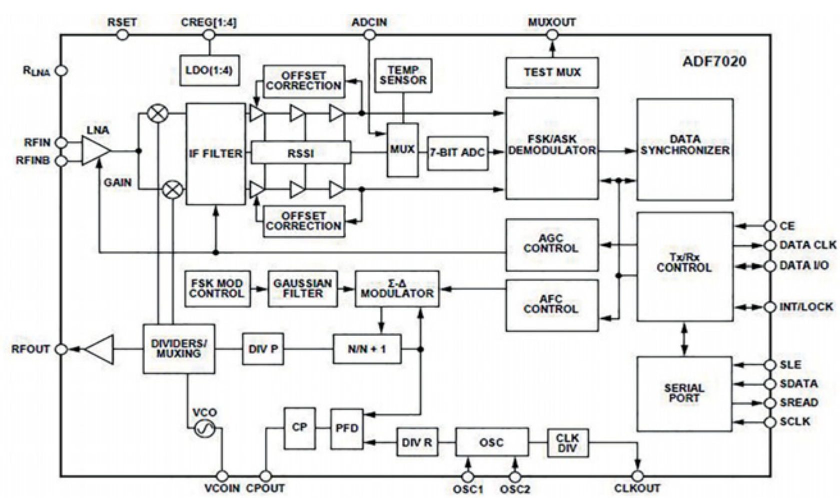

Figure 2: The ADF7020 integrates a temperature sensor and ADC with the transceiver for simple sensor links.

Square Peg, Round Hole

MYK DORMER IS A SENIOR RF DESIGN ENGINEER AT RADIOMETRIX LTD **WWW.RADIOMETRIX.COM**

It's an amazing time to be an engineer. Developments in semiconductor technology and the relentless progression of Moore's law have brought us an absolutely bewildering range of devices and solutions. Circuitry that used to occupy rack-frames, or even rooms, can now be realized on single boards, or even single chips, at a fraction of the earlier cost and power consumption, whilst new digital techniques make possible levels of signal fidelity, accuracy or bandwidth-compression that older analogue techniques could never approach.

In the arena of RF engineering we see similar advances: it is possible to integrate an entire signal path, from baseband input to the antenna, while digital signal processing methods allow us to implement almost all the functional elements of a radio design in firmware routines instead of actual hardware. Semiconductor-based frequency synthesis methods simplify signal generation, offering huge gains in flexibility and stability over traditional custom frequency crystal or free running oscillator-based approaches, while even the basic discrete transistors we still use now exhibit levels of gain, operating frequency, stability and noise performance that would have looked fictional even twenty years ago.

Unfortunately, in the "small pond" that is low-power wireless design, not everything is progressing relentlessly forward to a better future. An unfortunate side-effect of these increases in integration is that the devices are becoming more and more tied in to their specific application areas and less usable for other, more generic, tasks. For example, in the 1990s the local oscillator of a cellular phone was typically realized using a discrete VCO, controlled by a PLL chip and a crystal or TCXO reference. Those PLL devices were (and are still) also usable for a multitude of other frequency generation tasks in designs other than the parent cellphone.

The situation today is very different. Most cellphones use very high integration silicon, integrating the PLL, and probably the VCO as well, into an RF chip with most of the rest of the phone's signal path. The result is a smaller, cheaper phone, but the parts it is made from are no longer usable for any other purpose, which in turn has resulted in the older, "generic functional block" devices becoming obsolete as the manufacturers turn their attention (and finite manufacturing capabilities) only towards the newer, high integration, single-use parts.

> "It is getting harder to find "generic" PLL devices or intermediate frequency parts. Even basic parts like dual-gate MOSFETs, low-noise junction FETs, or even some RF gain blocks, are getting scarcer

For RF engineers working in the lower volume parts of the industry (low-power wireless telemetry modules sell in thousands, or tens of thousands; not the tens of millions that cellphones sell in) or in sectors the "spotlight" of the specifically tailored part hasn't landed on, a problem is starting to become evident. We still use conventional radio design techniques, with separate functional blocks, some realized with sophisticated integrated circuits, some with quartz parts and some with "old fashioned" discrete circuit design.

The supply of parts suitable for these tasks is beginning to dry up. It is getting harder to find "generic" PLL devices or intermediate frequency parts. Even basic parts like dual-gate MOSFETs, low-noise junction FETs, or even some RF gain blocks, are getting scarcer.

However, the purpose of this discussion is not to mourn the passing of the techniques that we need to build radios but to suggest methods and parts that we can use in the future:

- **Custom silicon:** The same high-integration techniques that the consumer electronics industries are introducing are also being offered by a number of custom and semi-custom IC suppliers. Currently the design costs, NRE charges and delivery times are, for small-run radio designs, prohibitive, but every year sees a reduction, and each generation of design tools gets easier for the non-specialist engineer to use.

- **Programmable devices:** Digital engineers have had programmable logic devices (PALs and their many descendants) available to them for decades. The industry is now beginning to see similar on-the-bench programmable functionality in analogue parts. (Admittedly these parts are still in their infancy, offering only simple "handful of op-amp" levels of sophistication, but with time – and Moore's law – we will see parts more useful to the RF designer).
- **Back to basics:** When implementing an RF circuit function (an amplifier, a mixer, an oscillator) and finding that the chip you would previously have used is no longer available, it is well worth considering a return to a traditional discrete component design. Current generation surface-mounted RF parts are small, very inexpensive and offer levels of performance orders of magnitude better than their ancestors – 5GHz-capable low-noise transistor in a $2mm^2$ footprint package can cost under 5p. Polishing up your rusty circuit design skills can yield some unexpected advantages.
- **Consider digital alternatives:** Low-end microcontrollers are improving almost by the month, and processing power vs power consumption figures can easily exceed one MIP per mA. It becomes possible to implement a fair range of functions, such as timers, delay elements, tone generators or decoders, or sequencers, in simple software routines which would previously have been thought of as a task for either an analogue design or a dedicated part. Simple programming skills can be as useful to the RF engineer as the more familiar lab test equipment.
- **Subversion:** Semiconductor suppliers introduce parts with very definite ideas as to what they are to be used for. An innovative RF engineer doesn't need to be so limited. In the same way that mobile phone PLLs found their way into a much wider range of low-power RF devices, the current generation of RF silicon, intended (for example) for automotive security or white-goods applications, can be used in a much wider range of applications. As an example: a single-chip ISM-band transmitter is (when looked at as a functional block instead of as an application-specific part) just a programmable frequency generator and could just as readily be used as a receiver's local oscillator, or as a decoder's clock source.

To summarize the point that I'm making here: it doesn't really matter what component parts an engineer has available at a given time, it is the fundamental engineering skill, understanding and imagination that define what can be achieved. ●

ANALOGUE TECHNIQUES FOR EXTENDING BATTERY LIFE

BY **KEVIN TRETTER** OF MICROCHIP TECHNOLOGY INC

Getting the maximum life out of a battery requires an understanding of three key factors: battery technology, digital power management and low-power analogue techniques. Whilst most designers are familiar with the strengths and weaknesses of different battery chemistries and digital power control, they may be less familiar with the role that low-power analogue techniques can play in extending battery life.

Battery Chemistries

One of the key decisions for designers of portable electronics is the choice of battery technology. The four main battery chemistries are alkaline, Nickel Cadmium (NiCd), Nickel Metal Hydride (NiMH) and Lithium Ion (Li-Ion), each with its own advantages and drawbacks.

Typically, a fully-charged alkaline cell will produce a voltage of around 1.5V. This voltage will decrease as the battery's energy is used, so that at 90% usage the voltage will have fallen to around 0.9V. The combination of relatively high capacity and high internal resistance make Alkaline batteries inefficient for high current-drain applications such as remote-control toys, camera flash units and power tools.

For these high-current applications, NiCd battery cells provide a very durable and low-cost option, offering a nominal voltage of 1.2V which drops to around 0.9V at the end of the battery life. The drawbacks are their relatively low energy-density and the presence of toxic metals. In addition, a periodic full discharge is necessary to prevent large crystals forming on the cell plates and affecting battery life and performance.

In contrast, NiMH cells are more environmentally friendly and deliver around 40% more energy density than NiCd battery cells. Their nominal voltage of around 1.25V drops to below 1.0V at the end of battery life. The disadvantages of NiMH batteries are a considerably higher rate of self-discharge and lack of durability, compared to NiCd, caused by cycling under heavy loads and extremes of temperature.

For most portable consumer electronics, Li-Ion is now the dominant battery chemistry. A fully-charged single Li-Ion cell has an open-circuit voltage of around 3.6V, decreasing to around 2.7V when fully depleted. The advantages of Li-Ion cells include lighter weight, higher cell voltages and, with Li-Polymer versions, the ability to be shaped. Another advantage is that the energy density of Li-Ion and Li-Polymer batteries continues to increase and is currently about twice that of a standard NiCd, whilst their costs decrease. The main disadvantage of this chemistry is the risk of explosion if overcharged. This valid safety concern means that some manufacturers are instead opting for NiMH chemistries, particularly where size and weight are not critical factors.

DC-To-DC Converters

An understanding of DC-to-DC converter architecture is essential for optimising the overall performance of a design and, typically, the choice will be between linear regulators, switching regulators and charge pumps.

Although there are several types of linear regulator, the most common used in battery-powered applications is the low dropout regulator (LDO). These use a P-channel pass transistor as a variable resistor with feedback to regulate a given output voltage.

In comparison, a switching regulator uses a diode, an inductor and a switch to transfer energy from the input and provide a given output which is configured in either a buck, boost or buck/boost topology. A buck regulator provides a regulated output

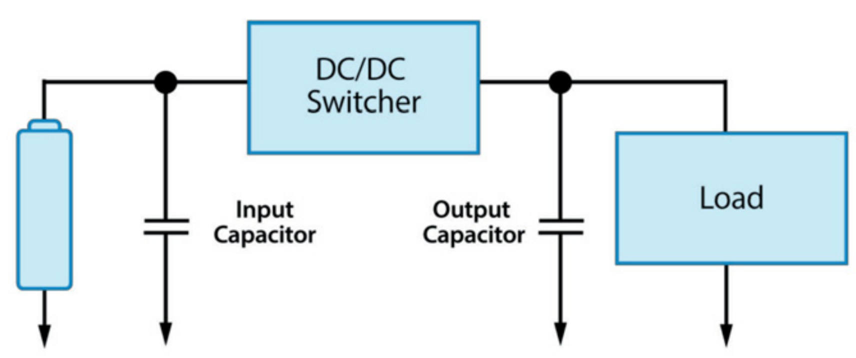

Figure 1: Placement of input and output capacitors for a switching regulator

voltage that is lower than the input voltage – similar to the function of an LDO; a boost switching regulator provides an output voltage higher than the input voltage; whilst a buck/boost regulator delivers a regulated output across a range of input voltages above and/or below that of the output voltage.

> Whilst most designers are familiar with the strengths and weaknesses of different battery chemistries and digital power control, they may be less familiar with the role that low-power analogue techniques can play in extending battery life

The third type of regulator, a charge pump, uses a capacitor as an energy-storage device and has switches to connect the plates of the capacitor to the input voltage. Depending on the circuit topology, a charge pump can double, triple, invert, halve or even create an arbitrary regulated output voltage. The use of charge and discharge capacitors to transfer energy means that a charge pump provides relatively low output current of no more than a couple of hundred milliamps.

Table 1 outlines the advantages and disadvantages of each of these DC-to-DC converter topologies; the choice of optimum topology will depend on the parameters of each application. For applications where long battery life is a priority, a highly efficient switching regulator may be the best choice; whereas in applications with a high level of electrical noise the choice would typically be a linear regulator. However, every application will need to focus on power-management circuitry if system performance targets are to be achieved.

DC-to-DC conversion offers a number of techniques for extending battery run-time. Figure 1, for example, shows the placement of input and output capacitors, in relation to the DC-to-DC converter. In this configuration, the switching regulator used to open and close an input switch can cause current surges on the input pin which can be minimised by using a large input capacitor as a charge buffer. This can affect battery run-time because, depending on the battery chemistry, the internal resistance may become significant and pulsing current from the battery can cause an appreciable voltage drop across the battery cell. A larger input capacitor, placed between the battery and the switcher, will reduce the instantaneous current draw, resulting in a voltage drop across the battery. By minimising these voltage drops, the run time of the battery can be extended before minimum battery cell voltage is reached.

In low-power applications, which spend a significant time in standby or sleep mode, it may not be necessary for the regulator to run at all times. Here, the use of a larger output capacitor to supply the low current required by the load can be more energy efficient. Cycling the regulator on and off boosts the capacitor charge as it is required.

Digital Power Management

Dynamic voltage scaling is another common technique for maximising battery run-time. When operated at a lower voltage, a digital load – such as a microcontroller – requires less current and therefore consumes less power. The drawback, however, is that operating a microcontroller at a low voltage can limit its processing speed and output capabilities. Dynamic voltage scaling enables the microcontroller to combine lower voltage and lower power consumption, when in standby or sleep mode, with a boost to a higher voltage level for processing or transferring information. This technique is used extensively in computing and many other battery-powered applications in which the microcontroller operates in different modes.

The amount of run-time versus standby or sleep for each application will also influence battery run-time. Whilst applications such as carbon dioxide detectors typically need to operate continuously, others can remain in standby or sleep mode until required. Examples of applications with intermittent operation include smart water meters, remote controls and photo-based smoke detectors.

Analogue Power Management

There are vast online resources dedicated to helping designers understand and manage digital power by using the different modes of operation offered by microcontrollers and, also, by turning its on-board peripherals on and off as required. The impact of running the microcontroller in a continuously active state, or putting it into sleep mode and then waking it for active operation, is also well documented.

When managing the power budget for analogue components, the choices may not be as clear.

Whilst it is still critical to use analogue ICs with the lowest active current for systems that use continuously active operation, applications which are duty cycled will also need to consider the settling time in relation to the current consumption. It may be that a higher-current, faster device may provide greater long-term efficiency than a lower-current alternative with a slower response time. ●

Parameter	Linear Regulator	Switching Regulator	Charge Pump
Efficiency	Low	High	Medium
Noise	Low	High	Medium
Output Current	Low to Medium	Low to High	Low
Step-Up Voltage	No	Yes	Yes
Step-Down Voltage	Yes	Yes	Yes
Solution Size	Small	Large	Medium

Table 1: DC/DC topology trade-offs

THEORETICAL AND EXPERIMENTAL STUDY

OF CAPACITIVE AND INDUCTIVE CROSSTALK

BY **OTHMAN B.K. HASNAOUI** AND **AKRAM GHARBI** FROM ENSIT (SCHOOL OF ENGINEERING) IN TUNISIA

One of the prevalent industrial concerns is electromagnetic compatibility (EMC) – the electromagnetic noise emitted by electrical systems has important consequences, since each system can be affected by it or affect another. So, EMC is the ability of an electronic or electric system to operate properly in its intended electromagnetic environment and, also, not be a source of pollution.

We have made an experimental setup for testing conducted emissions due to capacitive and inductive crosstalk (see Figure 1). We use the Tektronix TPS 2012B oscilloscope to display voltage noise generated by the connections, and the software "Open Choice Desktop" for the acquisition and recording of curves on a computer. We also use a low-frequency generator "GWINSTEK (GFG-8015G)" as a noise source.

Evidence Of Capacitive Crosstalk

In the case of capacitive coupling there is an interfering voltage capable of producing voltage noise; there is even capacitive coupling between the source conductor and the 'victim'. The workbench presented in Figures 1 and 2 shows this kind of coupling.

With the following equation, we can calculate the parasitic capacitance C_p:

$$C_P = \frac{\pi.\varepsilon_0}{\log\left(\frac{2.D}{d}\right)} \qquad (1)$$

where:

ε_0 is vacuum permittivity $= \frac{1}{36.\pi.10^9} = 8{,}85.10^{-12}$

D is the distance between electrical wires = 4 x 10^{-3}m

d is diameter of the conductors = 1.5 x 10^{-3}m

$C_{p,1}$ is the parasitic capacitance between the first wire (source of disturbances) and second wire (victim) as shown in the figures:

$$C_{P,1} = \frac{\pi.8{,}85.10^{-12}}{\log\left(\frac{2\times4.10^{-3}}{1{,}5.10^{-3}}\right)} = 0.03824nF/m \qquad (2)$$

$C_{p,2}$ is the parasitic capacitance between the interfering source and the third wire (see Figure 2):

$$C_{P,2} = \frac{\pi.8{,}85.10^{-12}}{\log\left(\frac{2\times8.10^{-3}}{1{,}5.10^{-3}}\right)} = 0.02704nF/m \qquad (3)$$

Figure 3 shows the parasitic voltage displayed on the oscilloscope, confirming the results of the equations.

Using a frequency generator, a 2MHz sinusoidal voltage is applied on the 'aggressor' wire. Clearly, the value of the parasitic capacitance decreases the further apart the wires are.

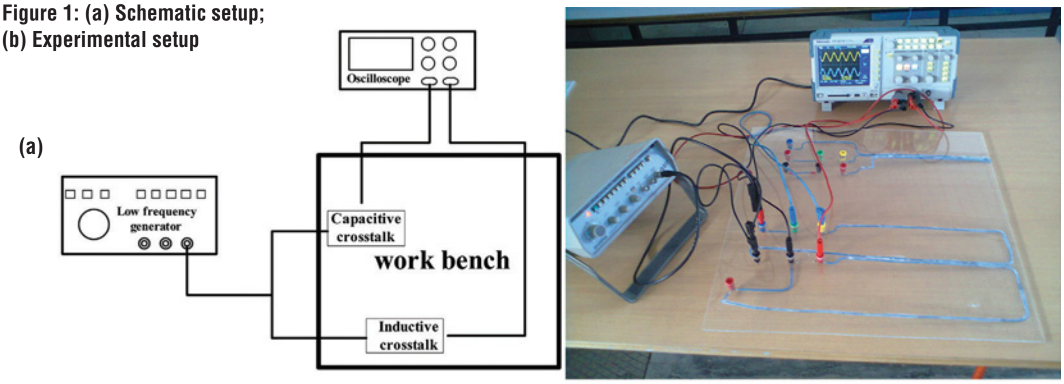

Figure 1: (a) Schematic setup; (b) Experimental setup

	Aggressor wire	'Victim' wire with screen	'Attacked' wire without screen	Percentage
Voltage level V(cc)	12.5	0.52	0.992	52.4%

Table 1: Shielding effect on capacitive coupling

Shielding Effect On Capacitive Crosstalk

We see the voltage noise caused by the source wire with the use of an oscilloscope, as shown in Figure 4. We find that the use of screened wire reduces the parasitic effects from 0.992V to 0.52V peak-to-peak (see Table 1).

If we increase the signal frequency applied to the source wire, the parasitic current that flows between the source and the victim increases (see Figure 5).

The interfering current is:

$$I_p = \frac{U}{R} \qquad (4)$$

where U is the voltage (peak) between terminals of the resistor R = 10kΩ.

For F = 1kHz, there is no induced voltage; for F = 10kHz, $I_p = \frac{75.10^{-3}}{10.10^3} = 7.5\mu A$; for F = 100kHz, $I_p = \frac{244.10^{-3}}{10.10^3} = 24.4\mu A$; and for F = 1MHz, $I_p = \frac{780.10^{-3}}{10.10^3} = 78\mu A$.

We conclude that with increased frequency, the capacitive interference intensifies.

Evidence Of Inductive Crosstalk

In the case of inductive coupling, there is a current in the ‘offending’ circuit likely to produce a current near the victim circuit. To illustrate this phenomenon we have developed an appropriate test-board (see Figure 7), which consists of two circuits: S_1, source of disturbance, and S_2, the victim loop. Inductance L which characterizes the current flow generated by the aggressor in the victim circuit is calculated with Equation 5:

$$\Phi = \iint B.dS = L.I_1 \qquad (5)$$

When a part of flux Φ crosses the second circuit S_2, this flux Φ_{12} is characterized by the mutual inductance M_{12}:

$$M_{12} = \frac{\Phi_{12}}{I_1} \qquad (6)$$

The voltage induced in the loop area S_2 is embraced by a magnetic field B. This phenomenon is expressed by the equation that results from Faraday’s law:

$$\underline{V_i} = -\frac{d\Phi}{dt} = -\frac{d(\int \vec{B}.\vec{n}.dS)}{dt} \qquad (7)$$

In our case the magnetic field is sinusoidal, so (7) becomes:

$$\underline{V_i} = jw.B.S.\cos(\theta) \qquad (8)$$

where θ is the angle between the normal $\vec{n}$ of the circuit and the magnetic field.

To the first circuit we apply an input voltage of 12.6V peak-to-peak; the noise voltage across the second circuit is 472mV peak-to-peak, as shown in Figure 8.

Inductive Crosstalk Tests

When we want to reduce the induced voltage V_i generated by the magnetic field B, generated in turn by the first circuit, we must take several factors into consideration.

Figure 2: Capacitive coupling test-board

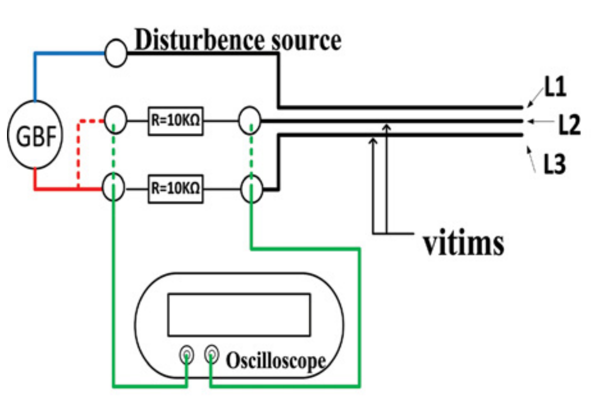

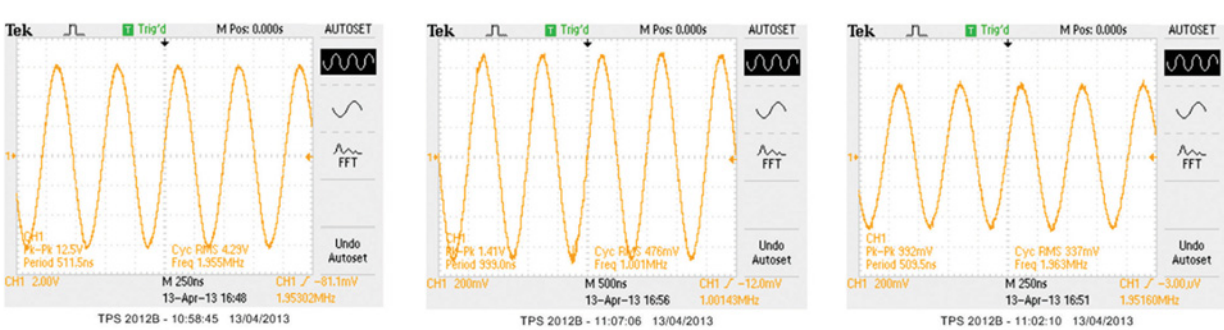

Figure 3: (a) Input voltage applied across the source wire (offender L1) V1 = 12.5V peak-to-peak;
(b) Voltage generated across the victim wire L2 (V2 = 1.56V peak-to-peak);
(c) Voltage generated across the victim wire L3 (V3 = 992mV peak-to-peak)

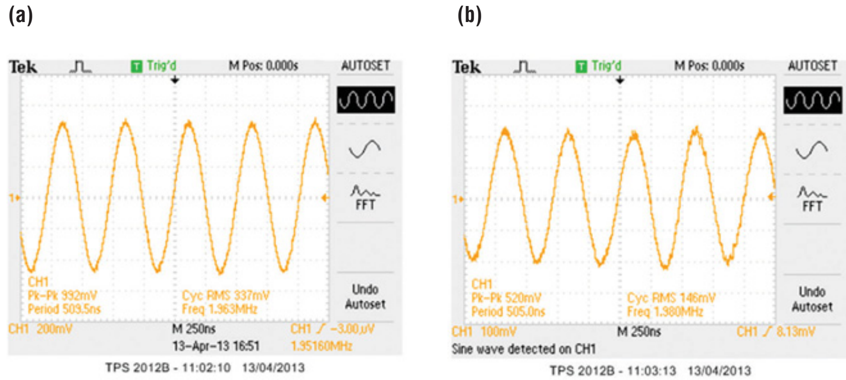

Figure 4: (a) Voltage generated by interference of the wire to the terminals of the victim L3 without screening; (b) Voltage generated by disturbances displayed to the terminals of wire L3 with screening

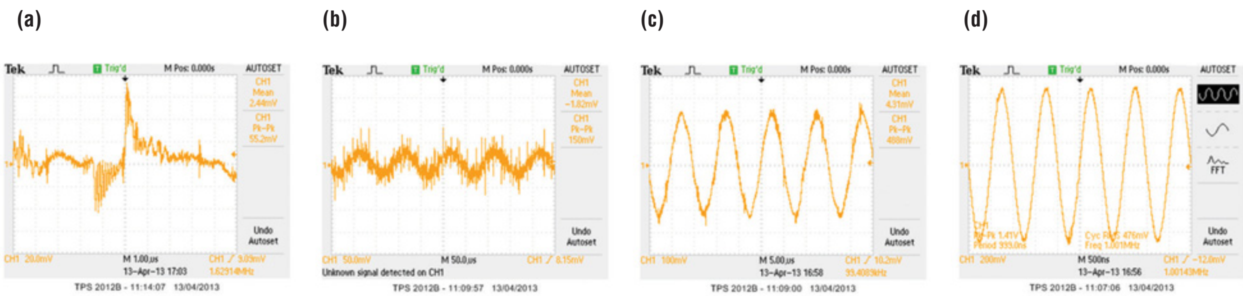

Figure 5: (a) Voltage across the victim wire for 1kHz; (b) Voltage across the victim wire for 10kHz; (c) Voltage at the terminals of the victim wire for 100kHz; (d) Voltage across the victim wire for 1MHz

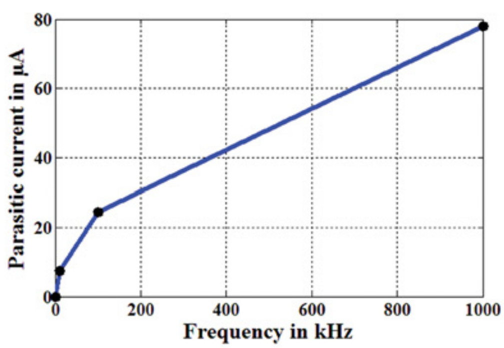

Figure 6: Parasitic current vs frequency source of noise

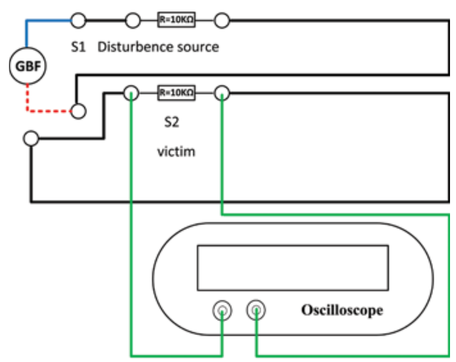

Figure 7: Inductive coupling test-board

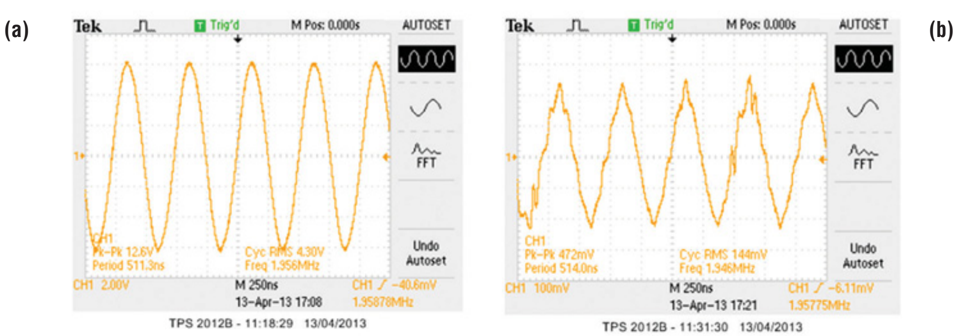

Figure 8: (a) Input voltage applied to the first loop Ve = 12.6V (peak-to-peak); (b) Induced voltage in the second loop Vi = 472mV (peak-to-peak)

$$V_i = j.2.\pi.fB.S.\cos(\theta) \quad (9)$$

We assume that θ = 0; so, factors that can reduce the inductive coupling are: magnetic field B, surface of the loop S and the frequency f of the disturbing signal.

As shielding we use 5mm-thick aluminium plate to reduce the magnetic field B, as shown in Figure 9. The use of an aluminium plate as a shield reduces the inductive crosstalk to a value of 186mV (peak to peak). Experimentally, to eliminate the parasitic effect of the inductive coupling we must choose the thickness of shielding depending on the intensity of the magnetic field.

One of the parameters in Equation 9 is the surface of the receiving loop, which we have to reduce to minimize the interference. The model we made (Figure 10a) has two circuits, equivalent to two loops of different surfaces, the first one being $S_1 = 322cm^2$ and the second surface $S_2 = 451cm^2$. According to the two previous curves, we can see that the induced voltage $V_i = 368mV$ of S_1 is smaller than that of loop S_2 ($V_i' = 472mV$).

Frequency is the most important factor in EMC. As frequency increases all the phenomena of electromagnetic incompatibility appear. If we vary the frequency, the inductive effect appears only above 1MHz; below that the oscilloscope displays only parasitics, as shown in Figures 11a and 11b.

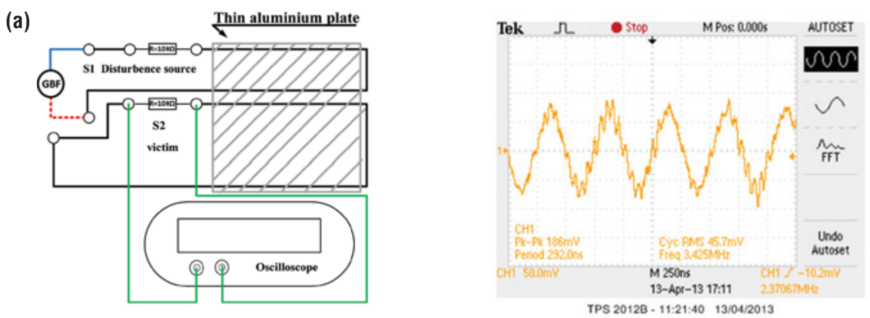

Figure 9: (a) Inductive coupling with a shield (aluminium plate);
(b) Induced voltage with a shield (aluminium plate) Vi = 186mV (peak-to-peak)

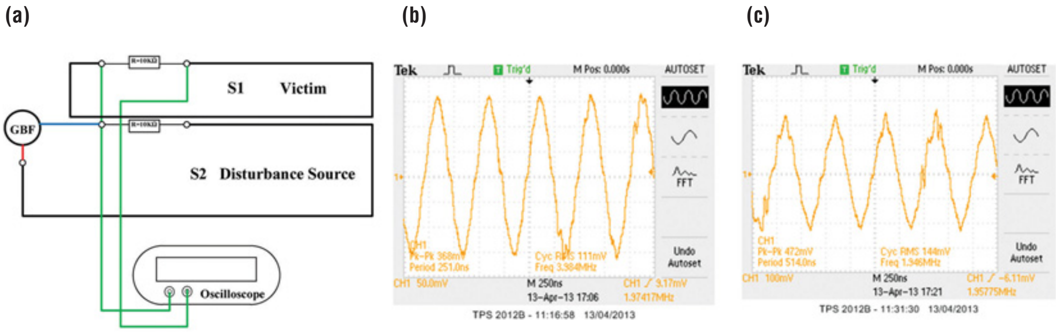

Figure 10: (a) Test board for reduction of surface; (b) Voltage Vi (peak-to-peak) measured on S1;
(c) Voltage Vi' (peak-to-peak) measured on S2

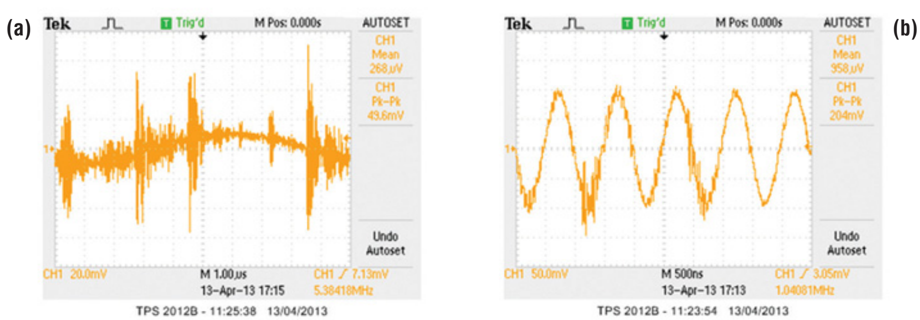

Figure 11: (a) Inductive coupling for f = 100kHz; (b) Inductive coupling for f = 1MHz (Vi = 204mV peak-to-peak)


WHO'S BEST TO DEPEND ON FOR THE PARTS I NEED?
DO THEY STOCK A WIDE RANGE OF PARTS FROM LEADING BRANDS?
NO
Don't settle for second best.
YES
We can offer around 500,000 parts from over 2,500 brands you know and trust.
IF I ORDER TODAY CAN THEY DELIVER TOMORROW?
NO
Don't risk it.
YES
We offer same-day despatch with free next working day delivery (conditions apply) on purchases above £20 (excl. VAT).
IS IT EASY TO FIND THE PARTS I NEED?
NO
Aaargh!
YES
Our website makes it simple and efficient to find what you need.
DO THEY HAVE GREAT CUSTOMER SUPPORT?
NO
Uh oh...not good.
YES
Our fast, friendly help and support team is only a call away.
DO THEY OFFER VALUE FOR MONEY?
NO
YES
Our one-stop, hassle-free approach saves you time and money, while regular price checks and large order discounts keep us competitive.
You can count on us for the parts you need
Beyond delivering on time, every time for over 75 years, RS Components delivers something you can't put a price on. Peace of mind.
uk.rs-online.com
RS

pF CAPACITANCE METER AND LABVIEW-BASED ACQUISITION

BY **PEIPEI HU** FROM THE SCHOOL OF ELECTRONIC AND ELECTRICAL ENGINEERING AT THE UNIVERSITY OF MANCHESTER, UK

Capacitance measurement plays a vital role in industry so any picoFarad (pF) capacitance measurement circuit can provide high sensitivity to very small capacitances and yet be insensitive to stray capacitances.

Typically, the range of measured capacitances is within 0.1-10pF, with a resolution of 1fF (0.001pF), making high sensitivity and reduced baseline drift significant parameters for the capacitance measurement circuit.

LabVIEW is a popular development platform from National Instruments (NI), offering an ideal environment for creating algorithms, designs, prototyping and interfacing of real-time embedded systems. This article focuses on a method that uses LabView's myDAQ module to connect to the measurement circuit and the user-friendly software interface designed in LabVIEW to accurately detect capacitances (see Figure 1).

Circuit Design

For applications such as imaging systems, it is essential to measure only the capacitance between the chosen pins, so the circuit should be immune to stray capacitances between earth and the measurement probe.

For our project, we chose the charge/discharge measurement circuit instead of an AC ratio arm bridge method which performs well at frequencies below 100kHz. The switching frequency of our circuit reached 2-4MHz, so the charge transfer section offers faster data rate with less complexity and matches the requirements for low baseline drift and high signal-to-noise ratio (SNR).

Figure 2 shows that the unknown capacitance is between S1, S2 and S3, S4. For one switching cycle, when S1 and S3 are closed, the capacitor C_x charges to V_c, with current flowing into CD1, generating a negative voltage, V1.

For the other half-cycle, when S2 and S4 are closed, C_x discharges, with current flowing into CD2, creating a positive voltage at the output V2.

Figure 3 illustrates the whole measurement setup using a basic charge transfer circuit. A crystal with frequency of 2-4MHz connects to a decade counter (CD4017), followed by D-type flip-flops (CD4013).

The successive charging/discharging current pulses in C_x are detected via a detector using an op-amp (LM248N).

Figure 4 represents the four input control-clock signals of the analogue switches CD4066, generated by the CD4013 D-type flip-flops. It can be seen that switches 1 and 2 are opposite and switches 3 and 4 are also inversed, with a delay between the two pairs.

Using Equation 1, we can derive the charge moved from C_x to the detector for a single charge/discharge cycle:

$$Q = V_c C_x \quad (1)$$

With the control of four clocks, charging and discharging repeat at a frequency f. Current I_m is generated by the charging/discharging cycle:

$$I_m = V_c C_x f \quad (2)$$

This current is picked up and smoothed by the detector, which gives a negative DC output voltage V1 when the clock cycle is charging C_x:

$$V1 = -R_f V_c C_x f + e_1 \quad (3)$$

Similarly, the positive DC output voltage V2 is produced when C_x discharges:

$$V2 = R_f V_c C_x f + e_2 \quad (4)$$

Figure 1: Capacitance measurement circuit and NI USB data acquisition

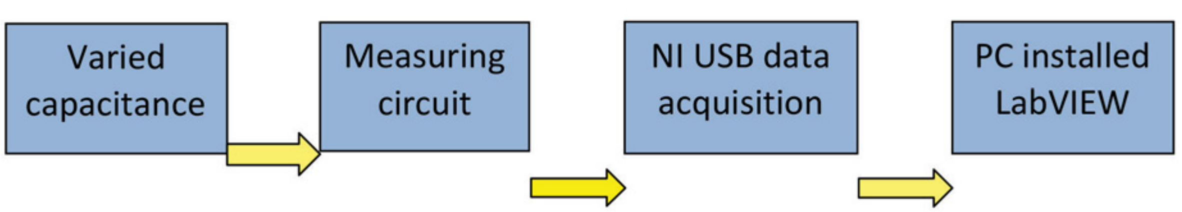

> LabVIEW is a popular development platform from National Instruments (NI), offering an ideal environment for creating algorithms, designs, prototyping and interfacing of real-time embedded systems

Figure 2: Basic capacitance-measurement circuit

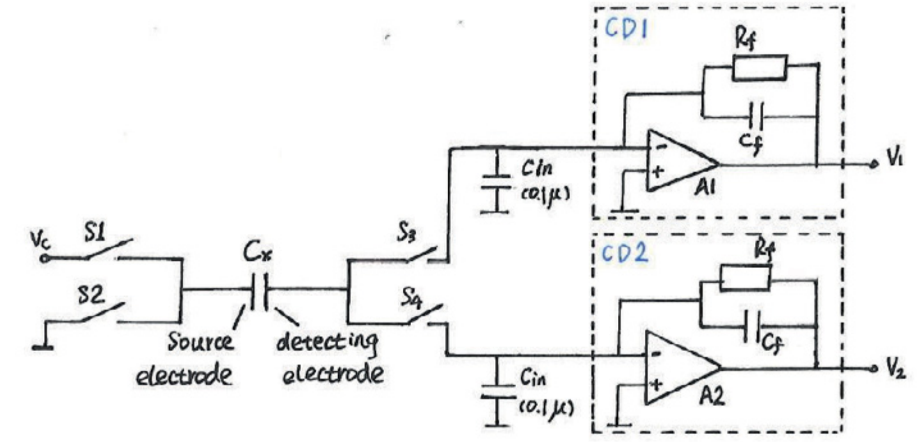

Figure 3: Measurement circuit detail

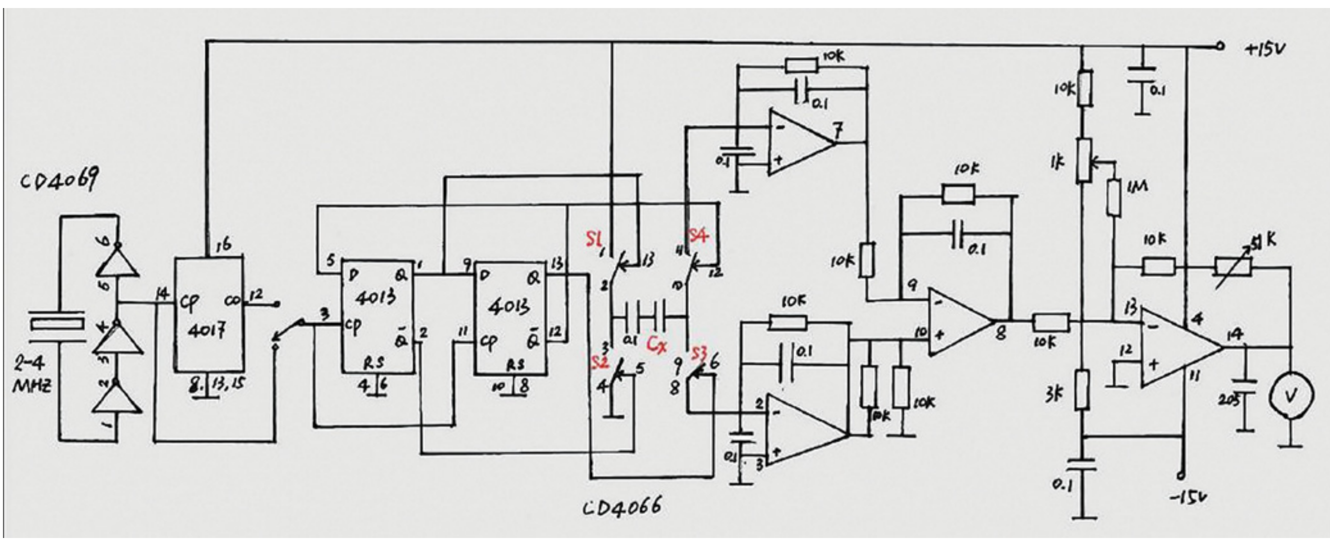

Figure 4: Analogue switches (CD4066) waveforms

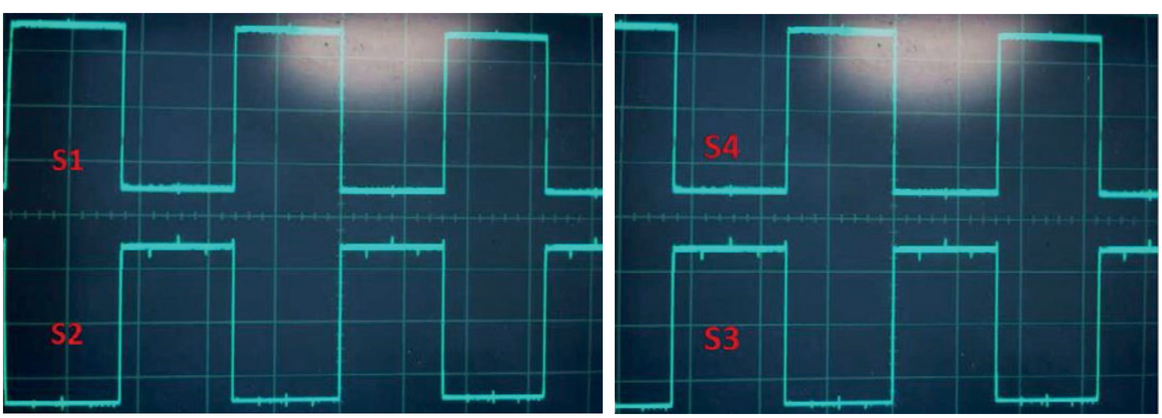

Figure 5: Measurement circuit PCB

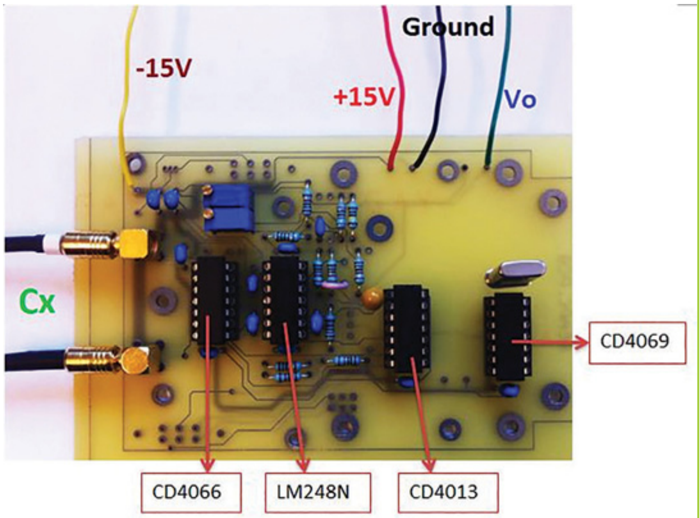

Figure 6: Front panel of the interface using My DAQ in LabVIEW

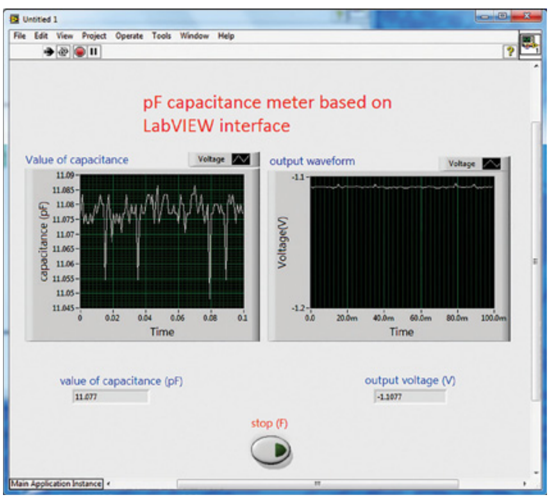

Figure 7: Block diagram of the interface using My DAQ in LabVIEW

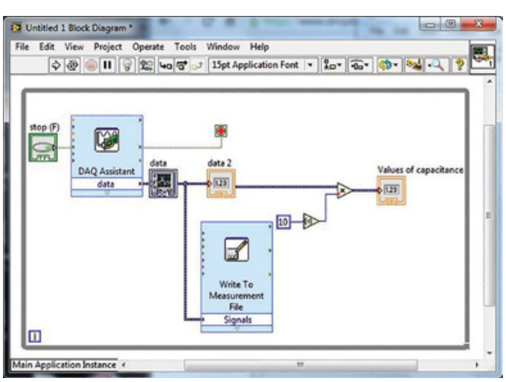

In Equations 3 and 4 the feedback resistor of the current detector is R_f , and e_1 and e_2 are output offset voltages caused primarily by the charge injection effect of the analogue switches (instead of the offset voltages of the connected operational amplifiers). Decoupling capacitances C' (0.1μF) safeguard the virtual potentials of the op-amps when the charging/discharging cycle changes very fast. When these cycles are changing, there is always low impedance between the input voltage and earth from the source electrode, and the virtual earth potential remains at the detecting electrode side, therefore there is virtually no effect to measure from stray capacitances.

The DC output voltage of the measurement circuit Vo is:

$$Vo = V2 - V1 = 2R_fV_cC_xf + e_2 - e_1 \quad (5)$$

According to Equation 5, it is easy to see the benefits of a differential structure: the sensitivity of the transducer is $2R_fV_cf$, doubled when compared to V1 or V2. Secondly, $e_2 - e_1$ shows the output setoff voltage being cancelled if the two op-amps are matched perfectly, with the equivalent charge injection effects and output offset voltages being almost the same. Because of this, a dual amplifier package is better than two single amplifiers.

It is found that the measurement circuit will be more sensitive with a larger feedback resistor; as with an operational amplifier, its dynamic characteristics are similar to a low-pass filter. The time constant is defined as $T_f = R_fC_x$. In this project, the circuit operates at a high frequency, so the time constant should be relatively small; the values of R_x and C_x are selected as 10kΩ and 0.1μF respectively, so the time constant is 1ms.

Advantages

There are several advantages of the charging/discharging method: First, there the inputs are the same in two halves of one cycle, such as the values of the feedback resistor R_f frequency f, coupling capacitance (0.1μF) and so on. They contribute to reducing the drift in differential circuits, and specifically achieving a low baseline drift of about 0.01pF/10°C when ambient temperature changes.

Second, the measurement can be very accurate, even at high frequencies (2-4MHz), due to the carefully selected time-constant. Third, the measurement of C_x is not affected by the other components. The resistance value of the CMOS 4066 analogue switch is below 125Ω and so can be ignored when compared to the feedback resistance (10kΩ). Also the turn-on/turn-off time of the switches is 20ns, a lot less than the time constant (1ms).

Figure 5 shows the PCB of our measurement circuit.

Designing The Interface In LabVIEW

Programming in LabVIEW is very important for designing the project's interface. Generally, text-based programming languages, such as Visual Basic, C++ and JAVA, follow a control flow type of program execution. Within the control flow, the execution sequence of programs is determined by the order of program components. However, programming in LabVIEW is different: it follows a data flow model to run virtual instruments (VIs). The node realises its function when all inputs are received by the circuit. The output data is produced by a node execution and it passes to the next node following the data-flow path. The execution sequence of the VIs and functions in the block diagram depends on the movement of data through the nodes.

Figure 6 shows the LabVIEW interface for this system. There is one stop button to enable stopping the measurement at any time. The scope shows the analogue voltage output from the PCB, and the value of the voltage can be read from the display "output voltage (V)". The value of the measured capacitance is observed by "value of capacitance" function directly.

It will be seen that there is still some noise in the waveform of the output voltage, because it is shown in a limited time range. Equally, the myDAQ module also contributes to the noise.

The Y-axis shows the value of the capacitance as between 11.045 pF and 11.085pF.

Figure 7 shows the program's sequence. In a loop, the data is transmitted to myDAQ, which is controlled by the stop button, with its output connected to a scope that displays the waveform. Because the output voltage from the PCB is negative and the sensitivity is 100mV/pF, values read from myDAQ are multiplied by -10 to show the capacitance in pF.

Test Results

Figures 8 and 9 illustrate the values of the measured capacitance. It can be seen that the calibration curves are very linear and the results are well matched at two frequencies (2.4576MHz and 3.2768MHz), a feature of a stray-capacitance-immune structure.

Baseline drift with time and temperature are regarded as main issues of system stability. No noteworthy baseline drift was found during the measurements, which were performed in a room where temperature variations were limited to ±2°C in one hour.

Figure 10 shows the project setup.

Figure 8: Measured capacitances at 2.4576MHz

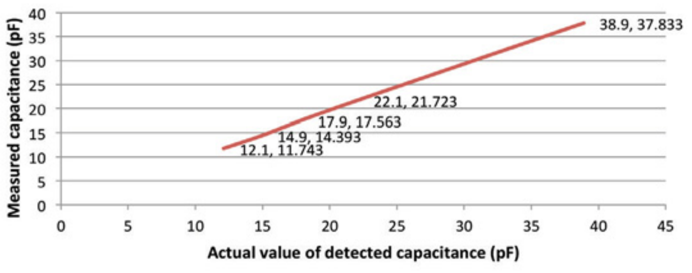

Figure 9: Block diagram of the developed sensor

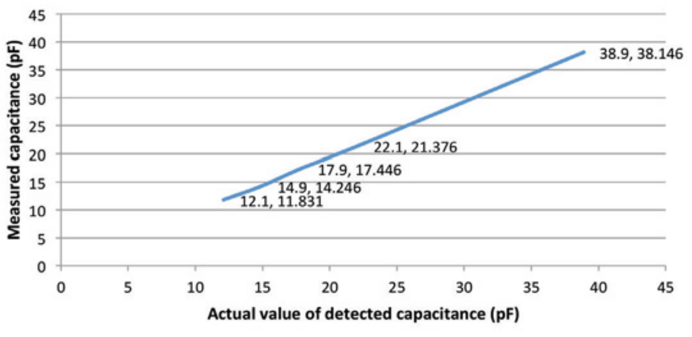

Power of ±15V is provided by a voltage source, the PCB is connected to the NI USB module, and both the value of the detected capacitance and the output of the measurement circuit are shown in the interface designed in LabVIEW. ●

Figure 10: The overall capacitance of the sensor

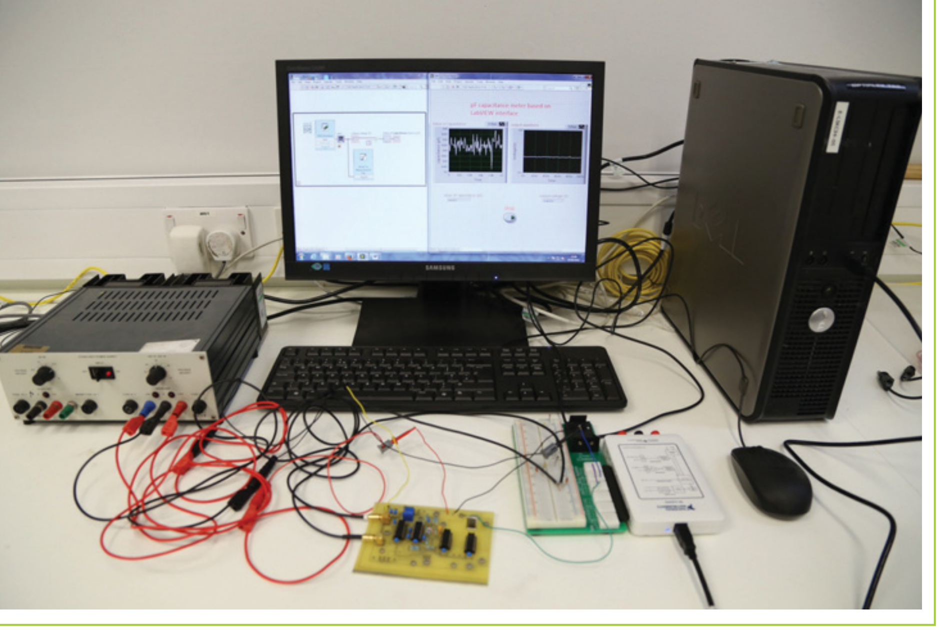

OVERVIEW OF THE ANALOG-TO-DIGITAL AND DIGITAL-TO-ANALOG DATA CONVERTER BASICS

BY **STOJCE DIMOV ILCEV** AND **IVAN SKORYK** FROM DURBAN UNIVERSITY OF TECHNOLOGY (DUT), SOUTH AFRICA

Today, it is almost impossible to find an embedded system without some form of digital to analog conversion or vice versa, where circuits convert analog signals into digital information, and the other way around – where analog signals are reconstructed from digital information.

Typically, an embedded electronic system is a microcontroller-based digital circuit, which cannot process or receive analog signals directly without their preliminary conversion into digital information, just as it is not able to form analog signals once the digital information has been processed by it.

The inter-conversion of signals is realized with analog-to-digital converters, or ADCs, and digital-to-analog converters, or DACs. These converters can be an integral part of a system with the microcontroller unit (MCU) or standalone devices. The illustration of the sequential analog-to-digital-to-analog conversion process is shown in Figure 1.

ADC Considerations

It's always important to analyze the end application so the right parameters and type of ADC can be selected for it.

An ADC's main characteristics to look out for are bandwidth (the frequency range that an ADC can measure), signal-to-noise ratio, or SNR (characterizing the accuracy of a signal measurement relative to noise), and dynamic range (characterized by the effective number of bits used for conversion which can be considered the resolution of an ADC).

The actual bandwidth of an ADC is characterized primarily by its sampling rate, which depends on the frequency of the digitizing signal. So, the higher the digitizing frequency of an analog signal to be made, the higher the sampling rate of the ADC must be.

The dynamic range of an ADC is influenced by many factors, but it is mainly determined by its Eeffective Number of Bits (ENOB), which can be also characterized as resolution, since the ENOB of an ideal ADC is equal to its resolution. The operation of an ADC is close to ideal when sampling at a rate greater than twice the bandwidth of the signal (ENOB is then considered equal to the resolution). When the sampling rate is less than twice the bandwidth of the analog signal, quantization errors may occur, and the bigger the number of quantization errors the lower the dynamic range of the ADC. In other words, the presence of quantization errors limits the dynamic range of an ADC; however, if the dynamic range exceeds the bandwidth of the input signal, the effects may be neglected.

> "The digital data link or communication bus has a tangible advantage in contrast to an analog transmission line in that digital data doesn't degrade when transmitted over long distances, whereas an analog signal can degrade and lose information

The type (architecture) of the ADC is determined by its implemented technical conversion principle in hardware (see Table 1 for various types). To some extent the SNR of an ADC depends on the type and so does its energy consumption.

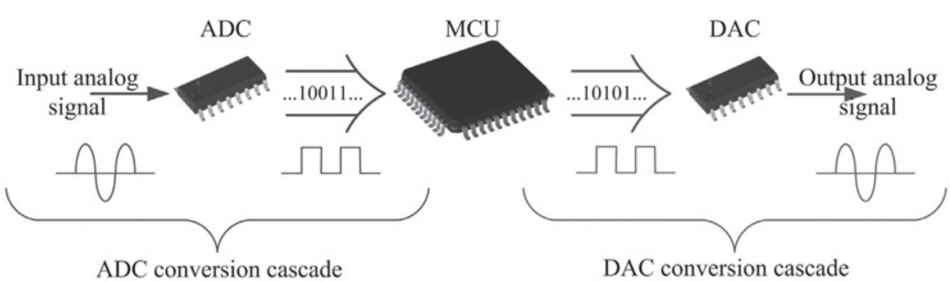

Figure 1: The analog-to-digital-to-analog processing sequence

DAC Considerations

DACs find many applications in systems and are in particular found in music players to convert digital data streams (audio/video) into analog audio signals, as well as in televisions and mobile phones among others. The most important aspects to consider when choosing a DAC are its power consumption, resolution, speed, accuracy, Total Harmonic Distortion (THD) and dynamic range.

The resolution is the number of possible output levels a DAC can reproduce. This is usually stated as the number of bits it uses, which is the base-two logarithm of the number of levels. Its resolution is related to the effective number of bits, or a measurement of the actual resolution attained by the DAC. The resolution of a DAC plays a crucial role in video colour depth and in audio bit-depth.

THD is a measurement of the distortion and noise, introduced to the signal by the DAC. It is expressed as a percentage of the total power of the unwanted harmonic distortion and noise that accompany the desired signal. This is a very important DAC characteristic for dynamic and small-signal DAC applications. Dynamic range is a measurement of the difference between the largest and smallest signals the DAC can reproduce, expressed in decibels, and is usually related to resolution and noise floor.

Other characteristics such as speed and accuracy mostly depend on the type of ADC (see Table 2).

ADC and DAC Communication Bus to MCU

An important part of the digital/analog design in which MCU and ADC or DAC might be used as standalone units is the digital communication bus. This can be either Inter-Integrated Circuit (I2C), Serial Peripheral Interface (SPI) or a Control Area Network (CAN).

The digital data link or communication bus has a tangible advantage in contrast to an analog transmission line in that digital data doesn't degrade when transmitted over long distances, whereas an analog signal can degrade and lose information.

The ADCs and DACs listed in this article feature an I2C or SPI module. The I2C module, used for relatively slow or low conversion-capacity ADCs and DACs, can provide data transmission at 400kbit/s. Devices with relatively high conversion capacity (such as for analog signal conversion) are featured with the I2C module, with data transmission up to 1Mbit/s.

The SPI module can provide much higher communication speed, up to 10Mbit/s, essentially determined by the MCU's clock speed.

Type	Applications	Devices and families	Main characteristics
Direct conversion (flash)	Precise and very fast signal processor.	MAX100 MAX104	Resolution 8 bits; Sampling rate up to 250Msps; High power consumption.
Pipeline	Fast signal processing; Precise power control.	MAX1200	Resolution 8 bits; Sampling rate up to 1Msps; Low power consumption.
Dual slope	Precision Analog Signal Processor; Precision Sensor Interface; High Accuracy DC Measurements.	TC5XX	Resolution 12 - 17 bits; Sampling rate up to 200ksps; Low power consumption.
Successive Approximation Register (SAR)	Data logging; Multi-zone Monitoring; Remote or Isolated Data Acquisition.	MCP30XX MCP32XX MCP33XX	The resolution 10 – 13 bits; Sampling rate up to 200ksps; Ultra low power consumption.
Delta-Sigma	Energy Metering and Power Measurement; Portable Instrumentation; Medical and Power Monitoring.	MCP34XX MCP35XX	The resolution 16 – 24 bits; Sampling rate up to 100ksps.

Table 1: General Information for ADCs

Type	Applications	Devices and families	Main characteristics
Pulse-width modulator (PWM)	Precise voltage regulator; Motor speed controller;	MCP47XX; MCP48XX.	Resolution up to 12 bits; Low power consumption.
Delta sigma modulator	High quality audio conversion; Signal formers.	CS4390.	Resolution up to 24 bits Medium power consumption.
R-2R ladder	Voltage calibrator; Precise voltage regulator; Low quality audio.	MAX501.	Resolution up to 12 bits; Medium power consumption.

Table 2: General Information for DACs

The CAN module is more specific in application. The CAN bus was primarily designed for the on-board network control of a vehicle, but has since found other applications, most notably in industrial environments. The maximum data transmission speed of the CAN bus is 1Mbit/s.

Converter Benefits

The operation of standalone ADCs and DAC units is very important in contemporary analog designs. These devices have the best quality-price ratio and can be easily purchased for enthusiast as well as commercial projects.

Their benefits can be summarized as follows:

- Separate units of ADCs and DACs allow a flexible design and layout of components on the printed circuit board, with a greater degree of freedom for the designer.
- Application of standalone ADC and DAC units allow updgrade of any microcontroller by adding them externally.
- Using a communications bus between the MCU and the other units allows up to 255 devices to be connected and maintained by a single MCU.
- There is a wide variety of ADC and DAC devices to choose from for any application, without imposing great requirements on the MCU, simplifying designs. ●

AMS POSITION SENSORS DELIVER BEST ACCURACY AT HIGH ROTATION SPEED

Discover Dynamic Angle Error Compensation (DAECTM) and win one out of 10 demoboards

ams' contactless position sensors offer best-in-class stray field immunity, high performance, superior durability and adhere to the most stringent safety requirements.

They are designed with ams' patented differential principle* which eliminates the effects of environmental factors such as stray magnetic fields, vibration, and misalignment. The portfolio includes a broad range of high performance rotary and linear magnetic position ICs suited for automotive, industrial and consumer applications.

The new "47 series" position sensors include the AS5047D, AS5147 and AS5247 with DAEC™ (Dynamic Angle Error Compensation), a technology developed by ams that eliminates the measurement error attributable to propagation delay.

- The AS5047D is ideally suited for industrial applications including robots and encoder modules.

- The AS5147 is an AEC-Q100 qualified part for automotive applications such as electronic power steering and pumps.

- The dual-die AS5247 (also AEC-Q100 qualified) is well suited for automotive applications requiring the highest level of functional safety compliance.

Check out the DAEC Video and scan this QR code. To win one out of 10 demoboards go to **www.ams.com/MPS**

About ams:

ams is a leading provider of high performance analog ICs and sensor solutions. ams' product range includes sensors, sensor interfaces, power management and wireless ICs for the markets consumer & communications, industry, medical and automotive. Based in Austria, ams employs 1,400 people globally.

www.ams.com

LIQUID-LEVEL SENSORS

PROFESSOR DOGAN IBRAHIM OF THE NEAR EAST UNIVERSITY IN CYPRUS DESCRIBES THE PRINCIPLES OF LIQUID-LEVEL SENSORS AND PRESENTS THE DESIGN OF A LOW-COST EDUCATIONAL LIQUID-LEVEL SENSOR CIRCUIT

The level of liquid in a container is one of the important parameters in any process industry. It is generally required to measure and then control the level of the liquid.

Many liquid properties may affect the decision of developing and using a liquid-level sensor. Electrical conductivity, buoyancy, acidity and electrical permittivity are some of the factors to be considered before developing or purchasing a sensor to measure the level of a liquid.

Sensor Considerations

Many different types of liquid-level sensors are used throughout industry. Some sensors are the contact type, which are immersed in the liquid, while others are contactless, where the sensor assembly has no contact with the liquid. Contact-type level sensors are like pressure sensors mounted at the bottom of the container; resistive wire, capacitive and electromagnetic sensors are placed vertically inside the container; float sensors at the top of the liquid; and so on. Examples of contactless-type level sensors are: capacitive sensors, ultrasound or microwave sensors, image sensors and others.

Typically, contactless sensors have longer lifetimes and can be used to measure the height of any type of liquid; on the other hand, they are comparatively more costly and may require various environmental precautions during measurement.

Contact-type sensors are low-cost, but cannot be used with corrosive liquids such as acids, or other strong chemicals or sticky liquids.

Figure 1: GSlevel M liquid sensor

Points to consider before choosing a liquid-level sensor include:

- Can the sensor be inserted into the tank, or should it be external?
- Can the sensor be in contact with the liquid?
- Should the level be measured continuously?
- What is the required accuracy of the sensor?
- What is the length of the tank?
- What is the operating temperature range?
- Does turbulence, foam, or vapour occur at the surface of the liquid?
- Is the liquid sticky or dirty?
- What type of output is required, i.e. digital, analog, voltage, current etc?

The GSlevel M (www.gillsensors.com) is a solid-state capacitive liquid-level sensor (Figure 1) available up to 2m long,

Figure 2: WIKA Model FFG sensor

primarily designed for marine applications where monitoring level of fuels or water is required. The sensor has ±2% accuracy and operates over a temperature range of -40ºC to +125ºC.

WIKA Model FFG (www.wika.co.uk) is a high-resolution level sensor (Figure 2) based on the magnetostrictive measuring principle where the position of a magnetic float is identified. The sensor operates from -200ºC to +200ºC and has a measuring accuracy of ±0.5mm.

GEMS UCL-510 (www.gemssensors.com) is a contactless ultrasonic level sensor (Figure 3) transmitter for corrosive or sticky liquids. The range of the sensor is 1.25m, with an accuracy of 3mm. The operating temperature range is -7ºC to +60ºC.

Molex capacitive fluid level sensors (www.molex.com) tend to be customized flexible circuits with pressure-sensitive adhesive sensors for non-metallic containers. As shown in Figure 4, the sensor is disposable, mounted outside the container. The accuracy is reported to be 95% when used in auto mode. The sensor provides multiple outputs such as USB and I2C, and discrete signals.

SICK (www.sick.com) guided radar liquid-level sensors (see Figure 5) are based on the principle of radar, where an electromagnetic impulse is generated and sent to the surface of the fluid to be measured. Part of the impulse is reflected back, and the fluid level is calculated from the time difference between the impulse sent out and the one received.

The LVCS liquid-level sensor (Figure 6) from the Deeter Group (www.deeter.co.uk) can measure liquid level up to a couple of meters. The standard resolution is 5mm, with the temperature range from -20ºC to +120ºC.

> “In practical applications it is easier and also more accurate to measure the capacitance and then find the relationship between the capacitance and the liquid height

Omega’s LVU40 series (Figure 7) ultrasonic liquid level sensor (www.omega.com) can measure levels in a range of 0.3-18.3m, with accuracy of ±0.25% and operating temperature range of between -40ºC and +60ºC.

Omega LVRD500 series radar level sensors (Figure 8) are long range (up to 15.24m) sensors with accuracies of ±0.25% and operating temperature range of -40ºC to +60ºC.

Omega capacitive level sensor probes are available for various ranges, types of liquids and operating temperatures.

The problem with commercially available liquid-level sensors is that they are quite expensive; for example, the LVDR500 sensor costs over $2,000. In small and educational liquid-level monitoring and control applications it is possible to develop a low cost, capacitance-based sensor using some basic parts. The sensor presented in this article is a microcontroller-based, low-cost, capacitive sensor used to measure the level of liquid in a non-conducting storage vessel.

Figure 3: UCL-510 liquid sensor

Figure 4: Molex capacitive sensor

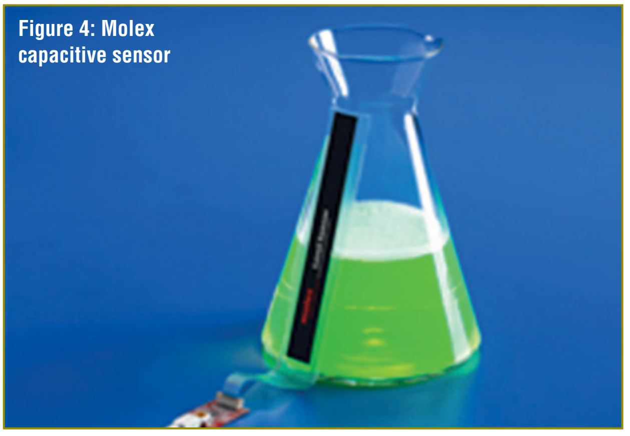

Principle And Construction Of A Low-Cost Sensor

Figure 9 shows the block diagram of the liquid-level sensor device. The sensor elements consist of a pair of aluminium foil papers stuck externally at opposite faces of the container, thus forming a parallel-plate capacitor. The physical shape of the plates is not important but in this example a rectangular shape is used.

An RC circuit is formed (here called the interface circuit) and the capacitor voltage is fed to a microcontroller. The microcontroller calculates the value of the capacitor by measuring the rise time of the RC circuit it is part of. Since the capacitance changes with the height of the liquid, liquid height is calculated and displayed on an LCD. Notice that in a normal liquid-level monitoring or control application it may not be necessary to use an LCD an LCD readout, except possibly for calibration or maintenance.

The capacitive sensor basically consists of a pair of series-connected capacitors, connected in parallel as shown in

Figure 5: Guided radar sensor

Figure 6: LVCS sensor

Figure 7: Omega LVU40 series sensor

Figure 8: Omega LVRD500 sensor

Figure 10, where C_p is the capacitance of the container membrane, C_w is the capacitance of part of the plates in the water and C_a is the capacitance of part of the plates in the air.

In practical applications it is easier and also more accurate to measure the capacitance and then find the relationship between the capacitance and the liquid height, and then use this relationship in a microcontroller-based circuit to calculate the liquid height.

Measuring The Capacitance

The value of the capacitor is measured by forming an interface RC circuit and then measuring the rise time of the voltage across the capacitor. The circuit diagram of the capacitor and the interface circuit are shown in Figure 11. A voltage divider circuit is formed using two 3.9K resistors and the mid-point voltage is fed to the positive input of an analog comparator inside the microcontroller. A 330K resistor is connected in series with capacitor C_x.

Initially, the capacitor is discharged through the 290-ohm resistor. At the beginning of the measurement a voltage is applied via output port RC0. The voltage across the capacitor rises exponentially and when it reaches half the applied voltage the output of the analog comparator changes polarity and this is detected by a program running on the microcontroller. The value of the capacitor is then calculated as described below and, finally, the height of the liquid is found.

The reason for using an analog comparator is so the capacitor value can be measured fast and hence accurately, since the capacitor values are very low (in the pF range) and the capacitor voltage cannot be measured by polling an input port. The advantage of the interface circuit in Figure 11 is that the capacitor rise-time is independent of the supply voltage V_i and it is not necessary to know the actual value of the supply voltage at any time.

The voltage across the capacitor rises exponentially, given by:

$$V_c = V_i\left(1 - e^{-t/RC_x}\right) \tag{1}$$

The output of the analog comparator changes sign when:

$$V_c = V_i / 2 \tag{2}$$

Thus, we get:

$$0.5 = e^{-t/RC_x} \tag{3}$$

or:

$$C_x = \frac{t}{0.6931471R} \tag{4}$$

But, R = 330K, giving:

$$C_x = 4.3718t \tag{5}$$

where C_x is in pF and t is in µs.

Figure 9: Block diagram of the developed sensor

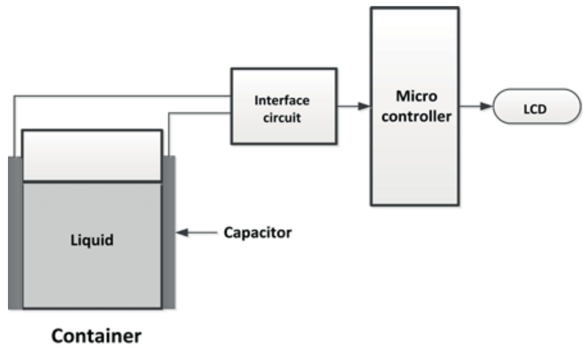

Figure 10: The overall capacitance of the sensor

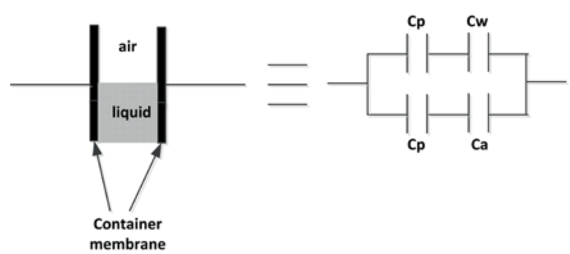

Figure 11: Circuit diagram of the sensor and interface circuit

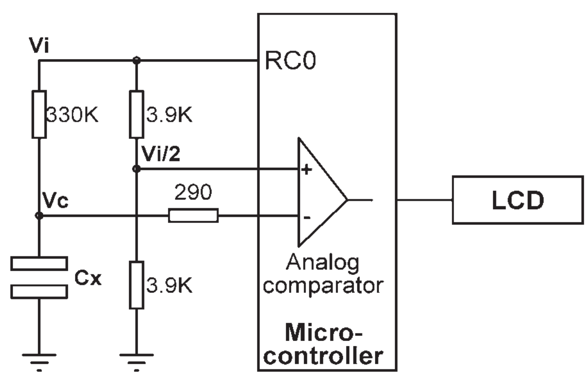

Figure 12 shows a graph of the measured capacitance against the height of the liquid. From this figure, the linear equation describing the relationship between the capacitance and the height is derived to be:

$$C_x = 5.25h + 16.5 \qquad (6)$$

In this project the capacitor plates had the following physical measurements:

Width = 11cm
Length = 26cm
Distance = 8.5cm

Combining Equations 5 and 6, we can calculate the height of the liquid using the following equation:

$$h = \frac{4.3718\,t - 16.5}{5.25}\ \text{cm} \qquad (7)$$

where h is the height in cm, and t is the time in µs.

Notice that in Equation 7 t is the time required for the output of the analog comparator to change polarity (i.e. for the capacitor voltage to rise to half the supply voltage). This can easily and accurately be measured with the microcontroller's built-in timer module.

Development Of The Sensor Device

Figure 13 shows the overall circuit diagram of the sensor sevice. Here, a PIC18F45K22 type microcontroller (www.microchip.com) is used, although any other type or model microcontroller could have been used. The main requirement is that the microcontroller support at least one timer module and one analog comparator module.

The microcontroller is operated from an 8MHz crystal. A 2 x 16 character LCD is connected to port B of the microcontroller. Port pin RC0 of the microcontroller provides supply voltage to the interface circuit during measurement.

The EasyPIC V7 development board (Figure 14) is used for development and testing. EasyPIC V7 (www.mikroe.com) is a complete microcontroller development board manufactured by mikroElektronika, supporting programming and in-circuit debugging, and consisting of many hardware components. The interface circuit was built on a small breadboard.

The PIC18F45K22 microcontroller contains two analog comparators. In this application, comparator 2 is used where RA1 (C12IN1-) and RA2 (C2IN+) are the comparator 2 inverting and non-inverting inputs respectively.

The software was developed using the mikroC Pro for PIC compiler. This is a powerful C compiler developed for the PIC16 and PIC18 family of microcontrollers. The compiled program can be simulated on the PC, or it can downloaded to the target microcontroller and in-circuit debugging tools can be used to test the overall system in real time.

Operation of the program is simple and is shown in Figure 15 in the form of a Program Description Language (PDL). At the beginning of the program various registers are declared, and the LCD and analog comparator module are initialized.

Actual height (cm)	Measured height (cm)
4.0	3.98
8.0	7.96
12.0	11.94
16.0	15.92
20.0	19.94
24.0	23.95

Table 1: Measured and actual liquid height

Figure 12: Measured capacitance and liquid height

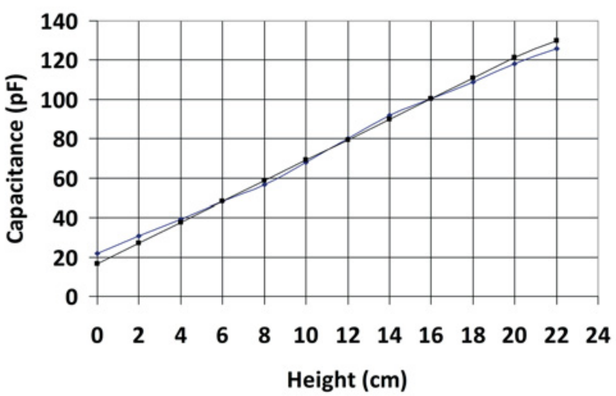

Figure 13: Overall circuit diagram of the sensor

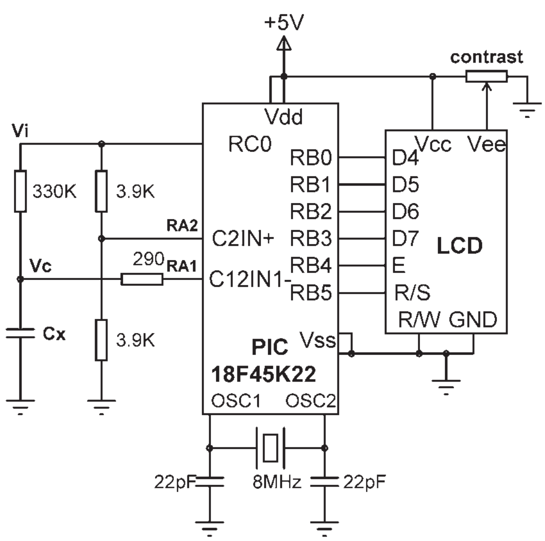

Figure 14: The EasyPIC V7 microcontroller development board

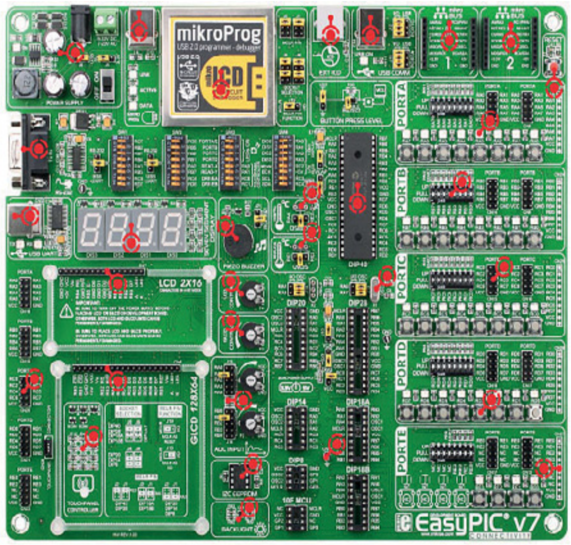

Timer 0 is configured for 16-bit operation with a basic count time of 1µs, so an accurate and easy measurement is possible. The main program executes in an endless loop where the capacitor is initially discharged by calling to function "discharge"; timer registers are cleared to zero, and the timer is started and voltage sent via port pin RC0 to start the measurement.

The voltage across the capacitor rises exponentially and the measurement stops when the analog comparator output changes polarity, i.e. when the capacitor voltage reaches half the supply voltage. At this point the timer is stopped and the timer count is converted into real elapsed time. The height of the liquid is then calculated using Equation 7. This process is repeated continuously with a one second delay between successive measurements.

Initializing Timer 0

The initialization of Timer 0 for a count of 1µs is as follows:

The clock frequency is 8MHz, thus the clock period is 0.125µs. The PIC18F45K22 microcontroller timer count-rate is given by:

$$\text{Timer count rate} = 4 \times (\text{clock period}) \times (\text{pre-scaler value}) \quad (8)$$

For a count rate of 1µs, the pre-scaler value is given by:

$$\text{Pre-scaler value} = 1\mu s/(4 \times 0.125) = 2 \quad (9)$$

The program in Figure 16 displays the capacitance and the liquid height in rows 1 and 2 of the LCD respectively.

Completed Sensor

The design of a low-cost educational capacitive liquid-level sensor circuit has been described here. The sensor element consists simply of a pair of aluminium foil papers stuck on either side of the external membrane of the container.

It was shown that a linear relationship exists between the height of the water in the container and the rise time of the voltage across the capacitor. A PIC microcontroller is used to measure the rise time and then to display the water level on an LCD. In real water-level monitoring and control applications the same microcontroller could also be used to control the overall system.

Tests were carried out using a container with the sensor mounted at the external membrane of the container. The height of water inside the container was measured using a ruler and also the developed system. Table 1 shows the measured and the actual height of water.

It is evident from Table 1 that the proposed design offers accurate results and the system can be used for educational water-level measurements. Accuracy of the sensor can be improved by increasing the microcontroller clock-frequency or value of the charging resistor. ●

Figure 15: PDL of the program

```
BEGIN/MAIN
        Declare variables and configure I/O ports
        Configure Timer 0 for 16-bit operation, 1µs time
        Configure analog comparator 2
        Initialize LCD
        DO FOREVER
                Clear timer registers
                Call "discharge" to discharge the capacitor
                Set RC0 = 1
                Start Timer 0
                Wait until comparator output changes
                Stop Timer 0
                Get Timer 0 count
                Calculate liquid height
                Display the capacitance on row 1 of LCD
                Display the height on row 2 of LCD
        ENDDO
END/MAIN

BEGIN/discharge
        Configure PORTA as digital
        Clear port pin RA1 to discharge the capacitor
        Wait one second
        Configure PORTA as analog
END/discharge
```

Figure 16: Program listing of the developed sensor system

```
// Define LCD-microcontroller connections
sbit LCD_RS at RB4_bit;
sbit LCD_EN at RB5_bit;
sbit LCD_D4 at RB0_bit;
sbit LCD_D5 at RB1_bit;
sbit LCD_D6 at RB2_bit;
sbit LCD_D7 at RB3_bit;

sbit LCD_RS_Direction at TRISB4_bit;
sbit LCD_EN_Direction at TRISB5_bit;
sbit LCD_D4_Direction at TRISB0_bit;
sbit LCD_D5_Direction at TRISB1_bit;
sbit LCD_D6_Direction at TRISB2_bit;
sbit LCD_D7_Direction at TRISB3_bit;
// End LCD-microcontroller connections

void discharge()
{
 ANSELA = 0x04;                  // Configure RA1 as digital
 TRISA = 0x04;                   // Configure RA1 as output
 CM2CON0.C2ON = 0;               // Disable comparator
 PORTA.RA1 = 0;                  // Set to 0 to discharge
 Delay_Ms(1000);                 // Wait 1 second
 ANSELA = 0x06;                  // Configure RA1, RA2 as analog
 TRISA = 0x06;                   // Configure RA1, RA2 as inputs
 CM2CON0.C2ON = 1;               // Enable comparator
}

void main()
{
 unsigned char TimerH, TimerL;
 unsigned char TxtC[15], TxtH[15];
 unsigned int Timerus;
 float capacitance, height;

 ANSELB = 0;                     // PORTB is digital I/O
 ANSELC = 0;                     // PORTC is digital I/O
 TRISC = 0;                      // PORTC output
 T0CON = 0x00;                   // Configure Timer0,16bit,Prescaler=4
 CM2CON0 = 0x89;                 // Configure comparator 2
 LCD_Init();                     // Initialize LCD
 PORTC.RC0 = 0;

 for(;;)                         // Endless loop
 {
 TMR0H = 0;                      // Clear timer high byte
 TMR0L = 0;                      // Clear timer low byte
 discharge();                    // Discharge the capacitor
 Lcd_Cmd(_LCD_CLEAR);
 PORTC.RC0 = 1;                  // Enable voltage to interface circuit
 T0CON.TMR0ON = 1;               // Start TMR0
 while(CM2CON0.B6);              // wait until comparator output changes
 T0CON.TMR0ON = 0;               // Stop TMR0
 PORTC.RC0 = 0;                  // Disable voltage to interface circuit
 TimerL = TMR0L;                 // Read timer low value
 TimerH = TMR0H;                 // Read timer high value
 Timerus = 256*TimerH + TimerL-20;   // Elapsed time in microseconds
 capacitance = 4.3718*Timerus;
 height = (4.3718*Timerus - 16.5) / 5.25;
 FloatToStr(capacitance, TxtC);  // Convert to string
 floatToStr(height, TxtH);       // Convert to string
 Lcd_Out(1,1,TxtC);              // Display capacitance
 Lcd_Out(2,1,TxtH);              // Display liquid height
 }
}
```

THE RAILWAY TO PRODUCT DEVELOPMENT

STEVE HUGHES, MANAGING DIRECTOR OF REO (UK), EXPLORES THE CURRENT CHALLENGES IN THE UK'S RAIL INDUSTRY AND PROPOSES CHANGES THAT WILL TAKE ITS TOP GAME WORLDWIDE

Despite carrying more passengers than ever, the UK rail industry is increasingly facing innovation challenges and market competition from more rapidly growing economies. This worrying trend can be attributed to a variety of sources: from an engineering skills shortage to poor practices in product development.

Walking down the aisle of a train at high speed, you may be forgiven for thinking that there's not a lot going on behind the scenes. With the quiet serenity of the cabin, the amusing pleasantries exchanged at the onboard coffee shop and the ever-shrinking journey times, it's not difficult to fall into a false sense of ease. Be under no illusion however, that this is the culmination of rapid development in the railway sector over the last fifty years.

Recent figures published by the Department for Transport show that, in 2013, UK rail passengers made 1.5 billion journeys, travelling some 36 billion miles. The majority of this growth has occurred over the last two decades, with the number of journeys having doubled since 1995.

It is evident then that, despite recent controversies surrounding the new HS2 high-speed line, train travel is an indispensable part of modern transport in the UK. The success of the rail network has, historically, been a key driver for the industrialisation of our towns and cities and a vanguard of economic growth.

However, it's not all plain sailing. The UK's rail infrastructure is ageing. Modern, electric multiple-unit (EMU) trains, which are capable of 145mph, are being limited to 125mph due to track limitations. If the UK is to keep pace with the technological innovation being undertaken in places such as China and continental Europe, concerted development in a few key areas is required. From safety, manufacturing processes and certification, to advanced analytical design methods and improved collaboration with education and research institutions, it is clear that rail has a long way to go.

Challenges

As a result of this, the rail industry faces a plethora of challenges, preventing significant innovation. These challenges can be grouped into three categories: environment, equipment and electrical.

The first challenge is the environment; the UK's natural environment and climate is wide and varied, from the vast lowland floodplains in the south, to the harsh mountainous regions in the north, from the sub-zero temperatures and flooding in the winter, to the hot and humid thirty-degree summers. This varied environment can put immense strain on both the train and any equipment exposed to the elements.

Developing the right equipment for this harsh environment is challenging to say the least. Products must be developed to withstand prolonged exposure to moisture and be acoustically dampened, and components must have the ability to endure the material stresses of constant high-speed shocks and vibrations.

The second challenge is equipment; the environmental challenge has over the years spawned numerous industry regulations for the development and innovation of equipment and components used in trains. These standards have attempted to increase safety and spur original equipment manufacturers (OEMs) into producing higher quality components by benchmarking against industry norms.

The rail sector has seen a multitude of regulations both at country and European level, including EN 45545, EN 60310 and EN 15085. They seek to address areas such as design analysis, materials selection, component performance, component assembly and arrangement, as well as quality control and fire safety. In addition to this, at the industry level, organisations such as the International Railway Industry Standard (IRIS) offer certification to over 90 companies worldwide, by auditing quality control, performing gap analysis and assessing OEM operations.

The third challenge is electrical. As railway technology has progressed, older, diesel-powered locomotion has been replaced with the modern electric multiple unit (EMU) technology. Whereas diesel technology used a single, diesel-powered locomotive carriage at the front or rear of the train and later moved to diesel multiple units (DMUs), EMU technology allows the self-propulsion of each carriage. This was achieved through the electrification of Britain's mainline network and is implemented through either a pantograph on an overhead line, or an electrified third rail. The AC power supply is then converted with an onboard traction transformer to provide each carriage with power.

The key benefit of using electric-powered trains instead of diesel is the fast acceleration and pollution-free operation. Furthermore, because they are quieter, electric trains can operate later at night without causing noise problems en-route. Electric trains offer better energy efficiency and reliability, ultimately improving the return on investment in the long term.

However, these benefits come at a price. Apart from the costly capital investment and maintenance of electric rail infrastructure, it can become difficult to provide a high quality, continuous power-supply to the network. For example, a traction transformer converts the overhead line voltage, which ranges from 15kV or 25kV, to a more suitable 0.7kV and 1.5kV.

The issue of power quality is one of the significant barriers to innovation in the drive toward the introduction of more electric trains. Bringing together a network of high-power equipment in such a confined space, inevitably leads to numerous issues such as electromagnetic interference, harmonic currents, telecommunication issues, flicker and heat. These problems raise the risk of component degradation and, ultimately, failure.

> “Recent figures published by the Department for Transport show that, in 2013, UK rail passengers made 1.5 billion journeys, travelling some 36 billion miles

The electric propulsion system requires the supply current to undergo a process of power conversion and high-frequency switching. Although this provides a usable power supply to the traction motors, it also introduces harmonics, the unwanted frequency components in electrical current. These harmonics can cause damage to components not rated to such high tolerances, as well as causing windings and transformers to overheat.

Large quantities of harmonics can cause instability in the supply known as electromagnetic interference (EMI). This interference can disrupt telecommunications equipment, as well as make the supply network prone to electrical fluctuations and surges, otherwise known as flicker.

Current Situation

So what is the industry doing to face these challenges? The European Union has set minimum standards for electromagnetic compatibility (EMC), to which electrical components must conform, before they are approved for commercial use.

Being a member state of the EU, Britain benefits from the standardised legislation and business synergies facilitated by the Single European Market, a trading bloc that seeks to guarantee the free movement of goods, capital, services and people. International partnerships, which have grown from this, have allowed British companies such as Virgin trains to source tilting train technology from Italy's Fiat Ferroviaria, for the Class 390 Pendolino trains built by France's Alstom.

Closer to home, trade associations such as GAMBICA and Power Electronics UK bring together OEMs, research bodies and legal campaigners to facilitate innovation through industry-leading market information, data analysis and cross-industry collaboration.

However, despite having a mature supply chain network, innovation in the engineering sector is increasingly stagnating. The recent Perkins review highlighted the engineering skills shortage in the UK and called for increased collaboration between government, engineering employers and educational institutions, to come together in developing engaging ways of turning today's youngsters into the engineers of tomorrow.

Modern, electric multiple-unit (EMU) trains, which are capable of 145mph, are being limited to 125mph due to track limitations

Best Practice

Whilst these measures provide a foundation for long term innovation at an industry level, there is a lot more OEMs can do to become more competitive in the market. Here at REO, our experience of building specialised components for the rail industry has taught us a few key lessons for success. By implementing certain steps, OEMs can build a true system of best practice.

Any approach at building a system of best practice requires a holistic perspective. In an era of increasing internationalisation, a responsive and integrated supply chain is vital in bringing together often disparate resources into a cohesive network with effective cross-border communication. This process starts with the consultation and conceptual design stages, moving through materials selection, design analysis and production planning, finishing with customer installation and after-sales service.

Too often, a lack of effective customer consultation leads to solutions unfit for purpose, creating a vicious cycle of poor product development. The key here is to break down the requirements capture phase based on core criteria; including safety, weight, space, cost and materials selection.

The key safety issues revolve around the environmental challenges already mentioned. As exposed elements and components are susceptible to ingress by dirt, debris and pollution, it is essential that ingress protection be prioritised for the development lifecycle. This also includes protection from moisture, as any wetness on windings and cables can cause short-circuits and thermal overloading.

As train companies struggle to compete with the ever-competitive prices of road and air travel, the push to minimise costs can often come at the expense of fire safety, with products being louder, heavier and less economical, taking up more space and ultimately failing to provide the most optimised solution.

The best way to address these factors is to undertake the best materials selection possible. A direct and focused analysis of the required material properties helps minimise costs, whilst maintaining performance and size/weight constraints. Inductors, transformers and winding materials have traditionally been available in aluminium, copper and iron. However, recent materials research has made possible the use of carbon fibre-reinforced plastics, as well as amorphous and nanocrystalline alloys, which offer superior magnetic properties.

Once a design has been finalised and the best use of materials considered, design analysis becomes possible. Design analysis is a virtualised form of product testing. Before the digital age, prototype designs would have undergone real-world testing in laboratories and in proving grounds prior to live placement. With the advent of high-powered computing, virtual testing of physical properties is now possible.

Finite Element Method (FEM) testing significantly shortens product development lifecycles, with improvements to digital prototypes now possible in hours rather than weeks and final development costs considerably reduced. Advanced FEM software applies simulated forces to the physical properties of a 3D model, highlighting areas of magnetic, thermal and structural weaknesses. These calculations allow engineers to tweak the design to eliminate potential hot-spots and stress points, and ultimately improve product life and performance.

Upon completion of the analysis phase, a prototype is produced, which undergoes destructive testing such as fire safety, shock and vibration, electrical performance, tolerance limits and EMC testing.

The above process demonstrates that high quality and sustained innovation is not immediately straightforward. Many OEMs will require some targeted business-process re-engineering, whilst others may need a complete process overhaul. Whatever the case, it is evident that a successful and integrated system of best practice is possible by following a holistic supply chain approach.

Having perfected this system over the last few years at REO, we have certainly benefited and, as a result, produce a higher-quality range of components. One such, recent development was the introduction of our REOLAB 420 (see box below), a high voltage direct current (HVDC) power supply used primarily for testing in railway engineering.

Food For Thought

The UK certainly has the potential to regain its position as the industry leader in railway technology. An integrated approach to supply chain networks, as well a concerted effort to increase collaboration and engagement with the engineers of tomorrow, is all that's required to bring the UK up to speed in the innovation of railway components.

So the next time you're at the onboard coffee shop buying snacks, spare a thought for the often unseen and unheard components that make your high-speed trip possible. ●

REOLAB 420

The REOLAB 420 is a three-phase DC high-voltage power supply. Ideal as an auxiliary supply, it is used for the development and testing of frequency converters in railway applications.

Input voltage for the unit is 3 x 400V line-to-line or 3 x 230V line-to-neutral, with an output voltage from true zero to 12,000 VDC. Output current is 2 x 20 – 300A and output power is 100-800kW as standard. Vector groups include Delta/Star/star/2 x B6U with a frequency range of 50/60Hz.

The REOLAB 420 complies with EC directive EN 61558-2-14 for power supplies with variable transformers. To further minimise the inherent dangers of working with high voltages, it offers an emergency-off circuit with external inputs and outputs as double-pole, potential-free contacts for emergency-off circuits and safety circuits.

As the unit is free of electromagnetic interference and maintains a constant residual ripple over the entire adjustment range of the DC output, it provides a control error as little as 1%. The output current is protected against short-circuit and overload and has been doubled at half the DC voltage selectable. Additional control of the supplementary equipment is attained by a 19" control unit, located away from the immediate vicinity of the HV supply unit.

Warning lights and additional connections for external warning systems increase unit safety. The REOLAB 420 has the ability to provide fast regulation of voltage variations and includes a built-in discharge circuit for the intermediate-circuit capacitor. This is further enhanced using an earth trip with a compressed-air drive to short out and earth the DC output.

THIS SERIES PRESENTS SOME SIMPLE ARDUINO PROJECTS. ARDUINO IS AN OPEN-SOURCE ELECTRONICS PROTOTYPING PLATFORM, BASED ON FLEXIBLE, EASY-TO-USE HARDWARE AND SOFTWARE

How To Prototype A Keypad and Display For An Arduino Project

BY **BROCK CRAFT**

The Arduino Keypad Entry System project has a lot of connections, so it's a good idea to prototype it first using a breadboard. After the prototype is built and tested, the breadboard can be fitted into an enclosure, or the circuit moved to a more permanent substrate, such as a stripboard.

The pin headers need to be soldered on to a keypad so the circuit can be inserted into the breadboard for testing, making things easier later when connecting a ribbon cable, either by soldering it to the pins or with a header socket soldered to the ribbon cable. After the pins are soldered on, the breadboard can be assembled.

The parts layout on the breadboard diagram shows the connections for the Rapid Keypad and Avago LED display. For different parts the connections will probably be slightl y different.

The components on the breadboard should be added as follows:

- Add the keypad.
- Insert the quad LED display on the left side of the breadboard.
- Add the 7219 display driver.
- Connect the keypad to the digital pins of Arduino, making sure the keypad pins for rows and columns correspond to the correct digital pins on the Arduino.
- Double-check the connections. It's easy to make a mistake.

It's always worthwhile to check the datasheet to be sure of the connections. Sometimes there may be extra pins on the unit that are not connected to anything; it depends on the manufacturer.

If a different unit is used, test its connectors first to determine how to connect it to Arduino.

At the time of writing, the datasheet for the Rapid Keypad part #78-0305 shows the wrong pinouts, which might have been changed by now.

Use jumper wires to connect the Max 72xx Driver IC to Arduino. This is rather simple, because you are using the SPI library to communicate with the IC, and it only needs three connections.

Add the capacitors to the breadboard. The 0.01 µF capacitor straddles the IC. To be most effective at preventing electrical noise from disturbing the IC, it needs to be as close as possible to the output pins 9 and 19. Straddling the IC is an easy way to do this. The 10µF electrolytic capacitor simply needs to be placed across the ground and power rails.

The 10µF is polarized, i.e. it operates correctly in only one direction. Make sure that the negative leg is connected to the negative power rail on the breadboard.

You may be tempted to omit the two capacitors, especially if you don't have them lying around your workbench. Don't! This can lead to erratic behaviour of the circuit and possibly permanent damage. They prevent noise on the power input and should be placed as close as possible to the V+ and ground pins of the IC.

Next, add the resistor between pins 18 and 19 of the Max 72XX Driver IC. This is used to limit current through each LED segment. The maximum current rating for the display determines the value of the resistors, which limit the amount of current flowing through each LED. The 72xx datasheet has a table that specifies the resistor values that should be used for the LED display.

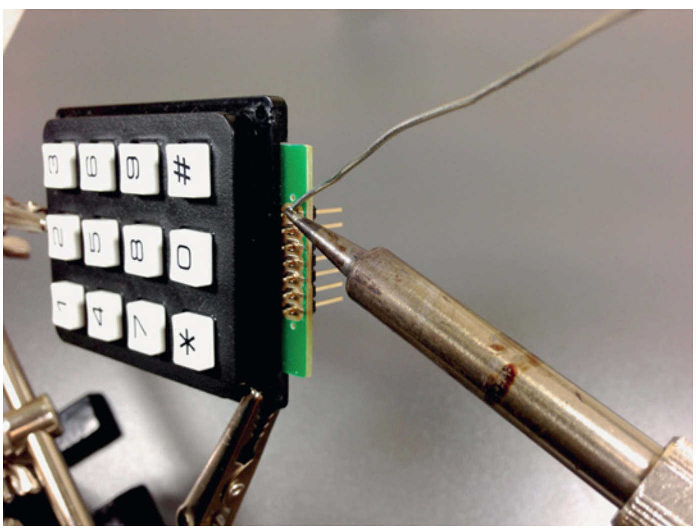

Figure 1: Assembiling the Rapid Keypad and Avago LED display

Arduino Digital Pin	SparkFun/ Rapid Keypad Pin	Keypad Row/ Column
2	7	Row 1
3	6	Row 2
4	5	Column 2
5	4	Row 3
6	3	Column 0
7	2	Row 0
8	1	Column 1

Table 1: Pin allocations

Figure 2: Connections for the Arduino setup

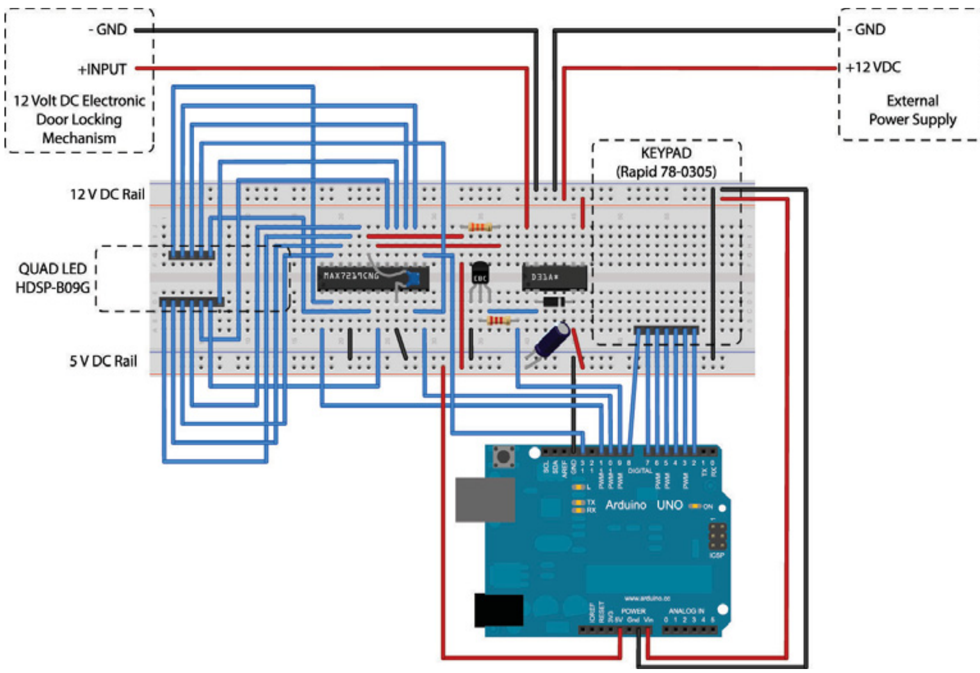

Arduino Digital Pin	Max 72xx Pin
10	1
11	12
13	13

Table 2: Connecting the Max 72xx driver IC to Arduino

The HDSP-B09G has a maximum of 25mA per segment at a forward voltage of 2.2V. Checking the table, this would indicate a resistor value of somewhere between 17KΩ and 28KΩ, but it's good to have a bit of a safety margin, so a 33KΩ resistor is specified. This works for both the Lite-On and Avago displays, but you might need a different value for a different display. Using a lower value could reduce the life of the LED or driver IC.

MAX 7219/7221	Lite-On LTC-4727JR	Avago HDSP-B09G
1		
2	1	12
3		
4		
5		
6	6	8
7	8	6
8		
9		
10		
11	2	9
12		
13		
14	14	11
15	11	10
16	16	7
17	15	5
18		
19		
20	13	4
21	5	1
22	7	2
23	3	3
24		

Table 3: Pinouts

Finally, connect the Max 72xx to the quad LED display; the way this should be connected depends on the pin layout. The schematic diagram doesn't show both displays. Pinouts for the quad LED vary by manufacturer, so in the diagram they aren't labelled by pin number. ●

More on this project, as well as other Arduino-related projects, can be found in the book 'Arduino Projects For Dummies' by Brock Craft.

WIN THE 'ARDUINO PROJECTS FOR DUMMIES' BOOK

Brock Craft is a lecturer in the Department of Computing at Goldsmiths, University of London. He drew extensively on his practical experience with Arduino to write '*Arduino Projects For Dummies*'. We have a couple of copies of this book to give away. To enter please supply your name, address and email to the Editor at svetlanaj@sjpbusinessmedia.com The winner will be drawn at random and announced at the end of the series.

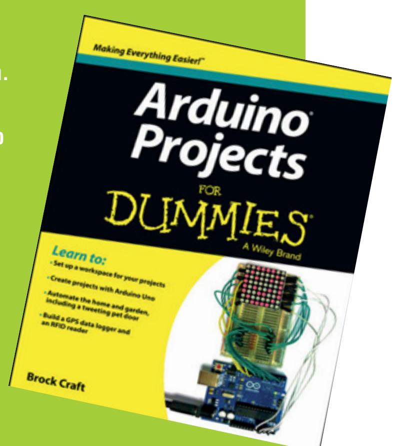

ASICs and ASSPs

MAURIZIO DI PAOLO EMILIO, PHD IN PHYSICS AND A TELECOMMUNICATIONS ENGINEER, PRESENTS THIS SERIES OF ARTICLES ON THE FUNDAMENTALS OF MICROELECTRONICS

Complex system-on-a-chip (SoC) designs are found in most of today's applications. During their design-ins, hardware designers must overcome many complex and challenging issues that relate to cost, time-to-market, performance, power, capacity, quality and IP integration among others.

In electronics, an Application Specific Integrated Circuit (ASIC) is typically customized for a particular use; for example, a circuit designed to operate in a digital recorder is an ASIC. Application Specific Standard Products (ASSPs), however, are in between ASICs and standard, off-the-shelf ICs.

An ASIC can integrate various components, such as bipolar transistors up to 80V, NMOS and CMOS logic (see Figure 1), JFETs, various sensors and others, implemented in a very large number of logic gates (in the millions). ICs of this type are called system-on-a-chip (SoC) and are programmed with languages such as VHDL.

ASIC/ASSP Design

ICs are made on a wafer, where circuits are built up with successive mask layers. The number of masks used to define the interconnect and other layers differs between full-custom ICs and programmable ASICs; see its typical design-flow in Figure 2, and a more detailed account of it is as follows:

- **Design Entry:** design through a specific language or by HDL or VHDL schematic description;
- **Logic Synthesis and Partioning:** creating a description of the logic cells used, their connections and ASIC division into sub-blocks;
- **Simulation of Pre-Layout:** first simulation to analyze the function of the project according to the initial requirements. This simulation is only a logical verification and doesn't take into account possible delays of signals that exist in the logic gates;
- **Placement:** the placement tool starts the physical implementation of the ASIC. The resulting placed-gates-netlist contains the physical location of each of the netlist's standard cells, but retains an abstract description of how the gate terminals are wired to each other. Typically, the standard cells have a constant size in at least one dimension that allows them to be lined up in rows on the IC;
- **Routing:** using the placed gates netlist and the layout view of the library, the router adds both signal connect lines and power supply lines. The fully routed physical netlist contains the listing of gates from synthesis, the placement of each gate and the drawn interconnects from routing;
- **Extraction:** calculation of resistance and capacity to assess the propagation delays;
- **Post-Layout Simulation:** analysis and simulation of the complete project.

Although an ASSP targets specific types of systems, in many cases it will be manufactured using ASIC technology but will ultimately be sold as a standard device type to numerous users. If the end user helped the chip maker design an ASSP, that user is typically given a market lead-time to use the device before it is made available to its competitors.

The primary advantage of the ASSPs or standard products is the ability to purchase the ICs immediately (most of the time) and get the system to market quickly. However, ASICs also allow the system producer to differentiate its product from the competition.

ASICs require very high volumes to be economically feasible (hundreds of thousands units), and the design process is extremely slow and inflexible. This means that products developed with ASICs are already old when they get to market.

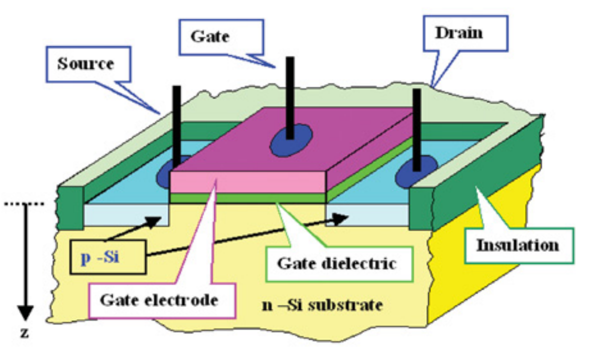

Figure 1: MOS transistor

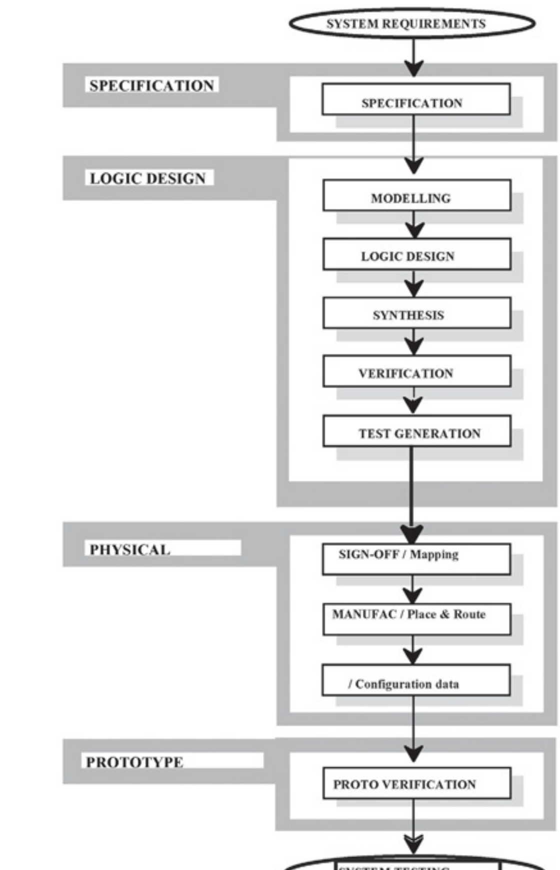

Figure 2: Flow of ASIC design

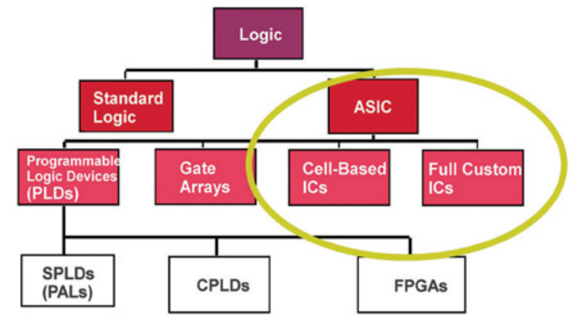

Figure 3: Asic design

An increasing number of consumer products (such as LCD TVs) adopt FPGAs to be able to embed the latest developments (algorithms) in the field. So FPGAs can give a competitive advantage by adding value and timeliness to the product.

There are several types of ASICs, one of which is the gate array, where diffused layers (i.e. transistors and other active devices) are pre-defined and wafers containing such devices are held in stock prior to metallization – in other words, unconnected. The physical design process then defines the interconnections of the final device. For most ASIC manufacturers, this consists on anything between two and nine metal layers, with each metal layer running perpendicular to the one below it. Here, non-recurring engineering (NRE) costs are much lower, as photolithographic masks are required only for the metal layers, and production cycles are much shorter, as metallization is a comparatively quick process (Figure 3). ●

KESTREL
Electronic Components Limited

Telephone: 01840-770028
Fax: 01840-770705
7 Gavercoombe Park Tintagel, Cornwall PL34 0DS
www.kestrel-electronics.co.uk

PIC18F13K22-I/SO	0.75	PIC16F1933-I/SS	0.64
PIC18F23K20-I/SS	0.78	PIC16F1933-I/SO	0.71
PIC18F24J10-I/SS	0.68	PIC16F1934-I/PT	0.81
PIC18F26K22-I/SS	1.28	PIC16F1936-I/SO	0.78
PIC18F43K22-I/PT	1.08	PIC16F1936-I/SP	0.93
PIC18F44J10-I/PT	0.95	PIC16F1936-I/SS	0.71
PIC18F44J11-I/PT	0.92	PIC16F1937-I/PT	0.81
PIC18F45K20-I/PT	0.96	PIC16F1938-I/SO	0.89
PIC18F45K22-I/PT	1.03	PIC16F1938-I/SS	0.82
PIC18F46K22-I/PT	1.31	PIC16F1939-I/PT	0.94
PIC18F64J11-I/PT	1.17	PIC16F1822-I/SN	0.35
PIC18F65J10-I/PT	1.19	PIC16F1827-I/SO	0.62
PIC18F65J11-I/PT	1.32	PIC16F1828-I/SO	0.63
PIC18F65J15-I/PT	1.33	PIC18F4520-I/PT	2.22
PIC18F65K22-I/PT	1.48	PIC18F6585-I/PT	4.55
PIC18F66J10-I/PT	1.37	PIC18F6621-I/PT	4.45
PIC18F67J11-I/PT	1.19	PIC18F6622-I/PT	3.35
PIC18F67K22-I/PT	1.79	PIC18F8722-I/PT	4.15
PIC18F87K22-I/PT	2.04	PIC18LF8722-I/PT	4.35
PIC12F629-I/SN	0.36	MCP2551-I/SN	0.38
PIC12F675-I/SN	0.42	M27C1001-10F1	2.44

We can also supply Maxim/Dallas, Lattice, Linear Tech
PLEASE VISIT OUR WEB SITE FOR FULL LIST

ENTRY-LEVEL INDUSTRIAL ETHERNET SWITCHES FOR HARSH ENVIRONMENTS

Belden has launched two new, robust, entry-level switches in its Hirschmann product range. The new SPIDER II 16TX EEC and SPIDER II 16TX/2DS-S EEC switches have a high port-density, thus offering a cost-effective means for implementing industrial Ethernet technology. Both SPIDER switches can be used to create flexible networking solutions for a wide range of industries, including automation, discrete manufacturing and transportation.

The switches have stable metal housing, can withstand extreme heat and cold, and are approved for use in environments with high risk of explosion. A second power supply may also be connected to further increase operational reliability. The switches, which can be mounted on a DIN rail and activated quickly via plug-and-play functionality, are suitable for connecting to the backbone or for networking linear and tree topologies.

The 16TX/2DS-S EEC variant offers two optical dual-speed uplinks, which can be equipped with Small Form-factor Pluggable (SFP) transceivers for different optical fibre types.

www.beldensolutions.com

DKFS: COMMON-MODE SMD CHOKES

Schurter has expanded its successful DKFS family of SMD chokes with a new horizontal version, which enables the use of very high-performance, compact chokes in low-profile assemblies.

Modern electronic circuits require components with the highest performance in ever smaller profiles. The new horizontal DKFS chokes are ideally suited for this purpose. Compared to vertical models, they have higher inductance with the same rated current. Thanks to SMD leads, they can be assembled using the same reflow soldering process as other components. Possible application areas for these chokes include switch-mode power supplies, DC and stepping motor drives and frequency converters.

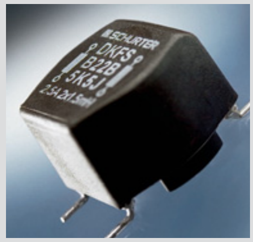

The rated voltage for DKFS devices is 250 VAC. These common-mode chokes are designed for temperatures of -40°C to +125°C. They will also continue to be available in vertical models as well as the new horizontal design. The DKFS series meets the requirements of IEC/EN60938 and is UL1283 approved.

www.schurter.co.uk

TWO-WIRE WHEEL-SPEED SENSOR IC WITH INTEGRATED CAPACITOR

The new A1688 from Allegro MicroSystems Europe is a Hall-effect sensor IC that provides a user-friendly solution for true zero-speed digital ring magnet and gear tooth sensing in two-wire automotive applications such as ABS braking systems.

The new device offers industry-leading performance in areas such as pitch deviation accuracy, consistent supply current distribution (better than six-sigma), low jitter and enhanced EMC performance provided by an integrated capacitor, which also reduces the requirement for external components.

The IC incorporates a dual-element Hall-effect sensor and signal processing circuitry that switches in response to differential magnetic signals created by magnetic encoders, or, when properly back-biased with a magnet, from ferromagnetic targets. A sophisticated digital circuit reduces magnet and system offsets, calibrates the gain for air-gap independent switch points and provides true zero-speed operation.

The regulated current output is configured for two-wire interface circuitry and is ideally suited to obtaining speed information in wheel speed applications.

www.allegromicro.com

HAN HOOD LINK SPEEDS CABLE-TO-CABLE CONNECTION

Harting has expanded its Han B industrial connector product portfolio with the addition of Han Hood Link, a new locking system that speeds cable-to-cable connection by allowing the connection of two standard Harting 16B hoods while simultaneously achieving an IP 65 degree of protection.

Key feature of the new connection is that it is made from a resistant elastomer which provides optimum protection against external mechanical forces, as well as good resistance to oils and gases. When used in conjunction with a specially contoured design, it achieves locking and sealing in a single action. As a result, housings can be quickly assembled and disassembled with minimal effort – all without tools.

A further product variant also permits housings to be locked together with both bulkhead and surface mounted housings.

This type of simple and robust locking element minimises the risk of connectors falling from heights and the associated damage to the locking device on impact.

www.harting.com

NEW JTAG OPTION FOR PEAK PXI TESTERS

A new JTAG/boundary-scan hardware interface is now available for the Peak Production family of PXI test systems.

The JT 2147/VPC from JTAG Technologies is a signal-conditional module that allows "ideal world" connections from JTAG Technologies PXI and PXIe DataBlaster high-speed boundary-scan controllers to the VPC (Virginia Panel Corporation) mass interconnect system supplied and used in Peak's configurable PXI-based functional testers.

Based on the highly successful QuadPod architecture from JTAG Technologies, the JT 2147/VPC has been specifically designed for connection into VPC's G20x or G14x 192-pin QuadraPaddle connectors and is fully compatible with the Peak system design.

The JT2147/VPC features four independent JTAG test access ports (TAPs) along with 16 static DIO (digital input/output) channels and 64 dynamic DIOS (digital input/output scan) channels. Adding boundary-scan capabilities to any board or system tester will increase fault coverage of interconnections, logic parts and in-signal passives, and reduce fixture costs due to test-point reduction.

www.thepeakgroup.com

DIGI-KEY'S FREE SCHEME-IT CIRCUIT DESIGN TOOL GETS UPGRADED

Global electronic components distributor Digi-Key Corporation recently announced new enhancements to the popular Scheme-it circuit design tool, available at no cost on the Digi-Key website.

Often thought of as an "idea generator", Digi-Key's Scheme-it design tool provides users with a simple, free-to-use way to record their circuit design idea in a shareable, electronic form.

The tool implements the entire Digi-Key catalogue, allowing users to design with actual parts available for immediate shipment from Digi-Key.

For more information, visit

www.digikey.co.uk/schemeit

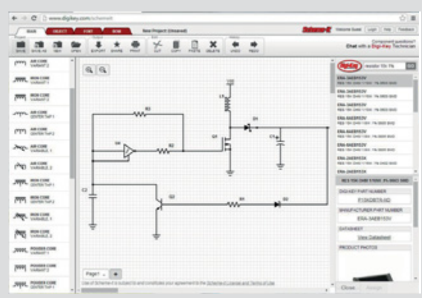

LATTICE MACHXO3 FPGAS WITH HIGH DENSITY I/O AVAILABLE FROM MOUSER

Mouser Electronics now stocks the MachXO3 Field Programmable Gate Arrays (FPGAs) from Lattice Semiconductor. These devices use a new packaging technology that eliminates bond wires, increasing performance while reducing cost, and resulting in increased gate and input/output (I/O) density while maintaining a small board-footprint.

The new MachXO3 FPGAs offer a very high gate density not usually found in programmable logic. These FPGAs feature low power-consumption with almost instant-on operation after power-up. Densities in this FPGA family range from 640 to 6900 Look-Up Tables (LUTs). In addition to LUT-based low-cost programmable logic, these devices also feature embedded block RAM (EBR) and distributed RAM. Internal phase locked loops (PLLs) reduce component count.

Enhanced flexibility in the I/O include drive strength control for driving external loads, slew rate control to compensate against high frequency oscillations, PCI bus compatibility, internal pull-up and pull-down resistors on the I/O pins and open drain outputs for driving loads.

www.mouser.com

NEW LYTSWITCH-2 ISOLATED LED-DRIVER ICS DELIVER MORE OUTPUT POWER

Power Integrations announced a new family of isolated LED drivers, called LYTSwitch-2, which delivers up to 12W of accurately controlled output power, substantially reduces component-count, resulting in simpler, smaller, more reliable LED lighting designs.

LYTSwitch-2 LED-driver ICs use primary-side control, resulting in cost-effective, single-sided PCBs with low component count. In addition, driver isolation allows the LEDs to be affixed directly to a metal heat-sink, avoiding the added expense of an electrically-isolating enclosure that is often required for non-isolated drivers. Accurate constant-current (CC) output tolerance across temperature (better than ±5% at both low-line and high-line voltages) reduces the need to over-design systems in order to meet requirements such as the US ENERGY STAR minimum-lumens-delivered specification, for example. Designs using LYTSwitch-2 ICs are also highly efficient – up to 90% in typical applications.

LYTSwitch-2 ICs protect the LED load from surges in line voltage, increasing bulb lifetime in regions where the mains voltage is subject to frequent peaks.

www.powerint.com

ROBUST, LOW-COST TX/RX FAMILY FOR POLYMER AND LARGE-CORE GLASS FIBRE SYSTEMS

OMC has launched the H19 range of low-cost optical transmitter/receiver devices for polymer and large-core glass fibre systems featuring a precision-machined metal ferrule which provides enhanced reliability for industrial applications. The range includes both single-channel devices for use with simplex fibre and dual-channel devices with duplex connectors facilitating transceiver operation.

Most connector systems for use with polymer fibre are produced almost entirely out of plastic, including the ferrule that attaches to the fibre. This provides a lower cost solution over metal connector systems, and can lead to reduced robustness and resilience when used in long-term industrial applications or other demanding environments.

OMC's H19 package benefits from the cost advantages of a high quality plastic housing. The design incorporates a precision-machined metal ferrule which provides a much higher level of precision and ruggedness over plastic-ferruled systems. The connector body also features twin metal side-plates which allow a four-point mechanical solder connection to the circuit board.

www.omc-uk.com

AVX EXTENDS HIGH RELIABILITY MLCC SERIES FOR COTS APPLICATIONS

AVX Corporation has added high-temperature X8R and X8L dielectric components to its high reliability APS Series multilayer ceramic capacitors (MLCCs) for commercial off-the-shelf (COTS) applications. Extensively tested using many of the MIL-STD test methods as used in MIL-PRF-55681, which eliminates the need for customer-specific drawings, APS Series MLCCs exhibit an ultra-low field failure rate of < 1ppb.

Now available in NP0, X7R, X8R and X8L dielectrics, in addition to a wider capacitance range than MIL spec parts and a variety of case sizes, voltages and termination finishes, APS Series surface mount MLCCs satisfy COTS requirements for higher CV demands and PCB space-saving requirements and provide high reliability performance in a broad range of critical applications, including military, aviation and telecommunications among others.

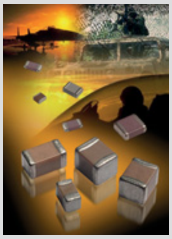

The APS Series MLCCs are available in six case sizes (0603 to 2220), six voltages (16-500V) and capacitance values of 10pF-22µF. They are also available with three capacitance tolerances (±5%, ±10% and ±20%) and four terminations.

www.avx.com

IC DESIGN CONSULTANCY SONDREL APPOINTS JOHN TINSON AS NEW GLOBAL VP SALES

System-to-silicon IC design consultancy Sondrel has appointed John Tinson as its Global VP Sales.

Tinson has over twenty years' director-level experience in fast-growing B2B technology companies and joins Sondrel from SPI Lasers, where he managed the commercial team that took the company from university spin-out to a £50m enterprise.

Announcing the appointment, CEO Graham Curren said: "Our company has grown rapidly over the past few years and now we are not only the largest IC design consultancy in Europe, but also a recognised force in the marketplace worldwide. John [Tinson] will be working closely with everyone to continue to drive Sondrel forward and achieve our ambitious sales goals."

Tinson holds a BSc in Physics from Birmingham University and studied business at Cranfield.

He said: "I'm thrilled to be joining Sondrel at this exciting stage in the company's evolution. Sondrel's business is now truly international, [and] I am looking forward to working with its multi-cultural teams and some of the most respected individuals in the industry."

www.sondrel.com

HARWIN APPOINTS DAVID RUMBALL AS EUROPEAN OEM SALES MANAGER

Harwin has appointed David Rumball as its European OEM Sales Manager. In this new role, Rumball, who can call upon nearly 20 years' experience in the electronic connector industry, will focus on developing strong relationships with end customers, pursuing and supporting design-in activity with OEMs.

"Our approach is to focus on the technology companies and to help them understand how our new products such as our Gecko 1.25mm pitch hi-rel connector family or our EZ-Boardware PCB hardware range comprising products that address EMC and test and cable management, can enhance their new product designs. It may be that the OEM customer's supply chain strategy dictates that they are serviced by our network of distributors, but it is critical that they are provided with direct support from Harwin – the manufacturer at the development stage."

An engineer by training, Rumball has a detailed understanding of Europe's hi-rel markets gained at senior positions at Amphenol.

www.harwin.co.uk

MICREL LAUNCHES NEW, CONFIGURABLE, FOUR-OUTPUT, LOW-JITTER, CRYSTAL-LESS CLOCK GENERATOR

Micrel introduced the DSC400, a four output crystal-less clock generator, last month. This is the first Micrel MEMS-based timing product launch which uses Micrel's proven PureSilicon MEMS technology to provide excellent jitter and stability while incorporating additional device functionality.

The device targets a broad range of applications including communications and networks; Ethernet 1G, 10GBASE-T/KR/LR/SR and FCoE; storage area networks, FC, SATA, SAS, FTTH EPON, 10G-EPON, GPON and 10G-PON; HD/SD/SDI video and surveillance; automotive; media and video and embedded and industrial, among others.

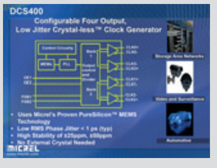

The DSC400 features low RMS phase jitter of less than 1ps (typ) and high stability with ±25ppm and ±50ppm options. It also offers high supply noise rejection of -50dBc and generates four outputs. Each output may be independently configured to be in LVPECL, LVDS, HCSL or LVCMOS format. With a wide frequency range of 2.3-460MHz, the device has excellent shock and vibration immunity (qualified to MIL-STD-88), high reliability and a wide supply range of 2.24-3.6V.

www.micrel.com

INTERCHANGEABLE (RT CURVE MATCHED) NTC THERMISTORS

ATC Semitec's SP interchangeable series is a range of NTC thermistors that offers very high precision (±0.2°C, 0 ~ 70C or better) at significantly lower pricing to that of existing interchangeable NTCs.

Readily available from stock, these new high-accuracy NTCs mean that now a wider range of users can cost-effectively achieve more accurate temperature control and thus more energy-efficient and comfortable working environments.

The main features of the SP thermistor range include the following:

R25 Values: From 1kΩ to 100kΩ;
Accuracy: ±0.2K from 0°C~70°C;
Temperature Range: -40°C/+150°C;
Fast Response;
2.6mm Bead Size.

Insulated and micro-miniature (0.5mm diameter) sensors are now available.

Contact the company directly for evaluation samples and ex-stock pricing.

www.atcsemitec.co.uk

IQD'S LAUNCHES NEW ±0.2PPB OCXO

IQD's new IQOV-164 series oven controlled crystal oscillator (OCXO) delivers exceptional frequency stability performance at ±0.2ppb over an operating temperature range of -20 to 70 degrees C. This new ultra-high-stability model can also be specified to operate over a wider -30 to 75 degrees C temperature range with only a minor drop in temperature stability performance at ±0.5ppb.

Available over a frequency range from 10 to 40MHz, this OCXO consumes a maximum of 7.0 watts during warm-up which takes only 3 minutes. Frequencies are available up to 100MHz with a lower stability of ±10ppb over -30 to 75 degrees C. Designed to operate from a 3.3V supply, the IQOV-164 is housed in an industry-standard 5-pin euro package measuring 36 x 27mm and 13.5mm high.

Output can be specified as either HCMOS, 15pF load or sinewave, into 50-Ohms load. Phase noise performance is typically -158dBc/Hz at 100kHz offset.

www.iqdfrequencyproducts.com

BULGIN LAUNCHES PREMIUM, VANDAL-PROOF PIEZO SWITCHES

Bulgin, an Elektron Technology connectivity brand, launched high-end, vandal-proof piezo switches, available in either aluminium or stainless steel. IP68 and IP69K rated, they have a robust one-piece construction, ensuring resistance to physical impact. Temperatures from -40 to +85°C can be accommodated, while environmental sealing guarantees weather and waterproof operation.

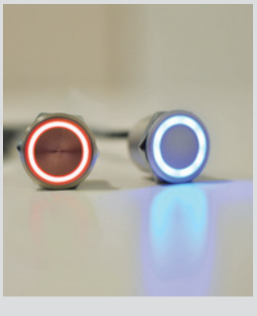

Customers have a choice of 16, 19 and 22mm hole diameter and ratings are up to 24V and 1A.

Dave Weaver, Product Manager for Bulgin, said: "Bulgin's high-end piezo switches have been carefully designed to withstand the most arduous uses, including heavy industry, electronics, public transport, military and defence, marine and food processing. We look forward to using this recently released product range to help meet the demands of our customers' challenging applications."

www.bulgin.com

PEAK GROUP CELEBRATES 30TH ANNIVERSARY

Letchworth-based supplier of automated test systems and accessories, The Peak Group, has celebrated its 30th anniversary on 1st of July.

Originally founded by Richard Bushell as a manufacturer of ATE in-circuit test fixtures, The Peak Group has diversified into a manufacturer of a comprehensive range of test equipment, from simple test boxes used by subcontract manufacturers to high-specification test racks and systems. An associated company, Peak Test Services, sells test probes and accessories from Chester-le-Street, County Durham.

Peak is a proven provider of automated test and measurement solutions, supporting every stage of the assembly process, from component testing to highly complex functional solutions. The company supplies innovative test solutions to a range of industries including the military, aerospace, rail, automotive, power generation and industrial electronics, supporting all aspects of the product lifecycle from prototype through to service and repair.

Peak offers intelligent integration of COTS ("commercial off-the-shelf") equipment with custom-designed mechanical, electronic and system software elements.

www.thepeakgroup.com

BELDEN INTRODUCES NEW EMEA-WIDE NETWORK CERTIFICATION PROGRAM

Belden has introduced an EMEA-wide certification program to help ensure that customers' industrial networks are reliable, adaptable and able to support growing control and information needs.

Belden is the first company in the industry to offer managers looking to install a new or significantly upgraded network a fully certified industrial network program to support and guide the process. Then, unlike ad hoc networks with partial product warranties, Belden certifies entire industrial networks, providing peace-of-mind and minimized downtime through enhanced warranties and dedicated customer support.

The program provides several key benefits, including dual expertise and counsel, flexibility for the future, a long-lasting confidence in the products, and personalized customer service, among others.

Belden partners with top system integrators in the industry, training them on best practices in network design, installation and testing and provide "Belden Certified" networks. At each step of the certification process, two sets of experts – Belden and an authorized provider – work to meet operational requirements and minimize areas of risk.

www.beldensolutions.com

OMRON LAUNCHES ITS MOST ACCURATE PRESSURE SENSOR

A new, highly-accurate, absolute pressure sensor from Omron Electronic Components Europe can detect height differences of as little as 50cm. Based on Omron's MEMs technology, the tiny sensor module can measure altitude, atmospheric pressure or water depth in wearable electronics, activity monitors, industrial and marine instruments and mobile phones and cameras.

This is the company's most accurate ever pressure sensor, providing readings relative to a perfect vacuum to ±6Pa. The module is just 3.8mm x 3.8mm x 1mm maximum, small enough to integrate into portable instruments. It provides an I2C output for easy integration into digital electronics.

The sensor uses piezo resistance in a full bridge circuit to detect pressure, and is fully temperature compensated giving an absolute temperature accuracy of ±2°C. The 2SMPB-01-01 offers the benefit of low power consumption of just 9µA typical, further simplifying its integration into portable and other battery powered electronic systems.

http://components.omron.eu

SENSIRION EXPANDING ITS SOFTWARE CAPABILITIES

Sensirion became the first company in the world to integrate a humidity and temperature sensor in a smartphone, enabling it to measure ambient temperature and humidity. The primary focus was not only on the development and production of the world's smallest humidity and temperature sensor, but also on the implementation and integration of the sensor. The company is increasingly developing as a software provider and as part of this effort, Sensirion has taken over the cloud business of Koubachi AG, strengthening its position in the internet of Things economy.

The Internet of Things, smart homes and wearables will be at the heart of the new economy, for which the basis is in intelligent sensor technologies and their integration into devices. Sensirion is the only company to offer the technology and its implementation from a single source, working closely with global smartphone manufacturers.

www.sensirion.com

PANASONIC'S HAS A NEW RANGE OF 'TOUGH CONTACT' BOARD-TO-BOARD CONNECTORS

Panasonic offers a range of 'tough contact' board-to-board connectors, which offer benefits such as improvement in resistance to corrosion, improvement in insertion/removal durability, improvement in contact reliability for digital signals, and influence of solder is controlled in both contact and spring parts. The range also offers 10-160 pin contacts, 0.8mm-0.2mm contact pitch and mating height as low as 0.6mm.

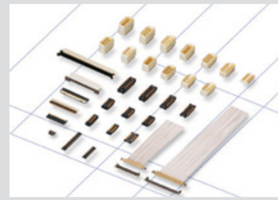

Anti solder-rise efficiency has been increased due to the NI-Barrier. Exposed nickel is placed on the mid parts of the socket contacts, which while being ultra low in profile prevents solder rise. In addition there's improved resistance to corrosion by gas due to porosity treatment. This treatment consists of coating the contact surface with a very thin film to seal pinholes in the gold plating.

A V-notch technology improves contact reliability; utilising the contact edge for the main contact area contact pressure has been increased dramatically.

www.panasonic-electric-systems.co.uk

PROTEUS 25

1989-2014

Pioneering Electronics Design Software

1989 Autorouter added to PCB for DOS
1990 Schematic capture added

1991 World 1st schematic capture for Windows®
1992 Topological route editing
1993 Fully integrated circuit simulation
1994 Rip up and retry autorouter
1995 Shape based power plane support

1996 True mixed mode SPICE simulation
1997 Interactive simulation
1998 PIC® microcontroller simulation
1999 8051 microcontroller simulation
2000 World 1st MCU co-simulation

2001 Language support for MCU simulation
2002 Electra adaptive shape based router
2003 World 1st 32 bit MCU support with ARM®-7
2004 Integrated Proteus VSM and MPLAB™
2005 Redesigned GUI across Proteus Suite

2006 3D visualisation engine
2007 World 1st USB simulation
2008 HDL support in simulation
2009 Shape based autorouter included
2010 VSM Studio IDE introduced

2011 Design rule aware manual routing
2012 ARM® Cortex™-M3 MCU simulation
2013 New application framework

2014

- NEW Project clips enable re-use of blocks of circuitry inside a project across multiple projects
- NEW Dynamic teardrop control including per pad override
- NEW Integrated Arduino™ toolchain with VSM Studio and common Arduino™ shields
- NEW Library import tools (BSDL,PADS ASCII)
- NEW New Project notes module for generic entry of notes and reports
- NEW Major upgrade to BOM module to improve physical output and simplify styling
- NEW Improved support for paste, solder, fanout and stitching vias during footprint creation

labcenter Electronics www.labcenter.com

Labcenter Electronics Ltd.
21 Hardy Grange, Grassington, BD23 5AJ.
Tel: +44 (0)1756 753440, Email: info@labcenter.com
Registered in England 4692454